iScience

CellPress
OPEN ACCESS

Article

5-HT_{1A} and 5-HT_{2B} receptor interaction and co-clustering regulate serotonergic neuron excitability

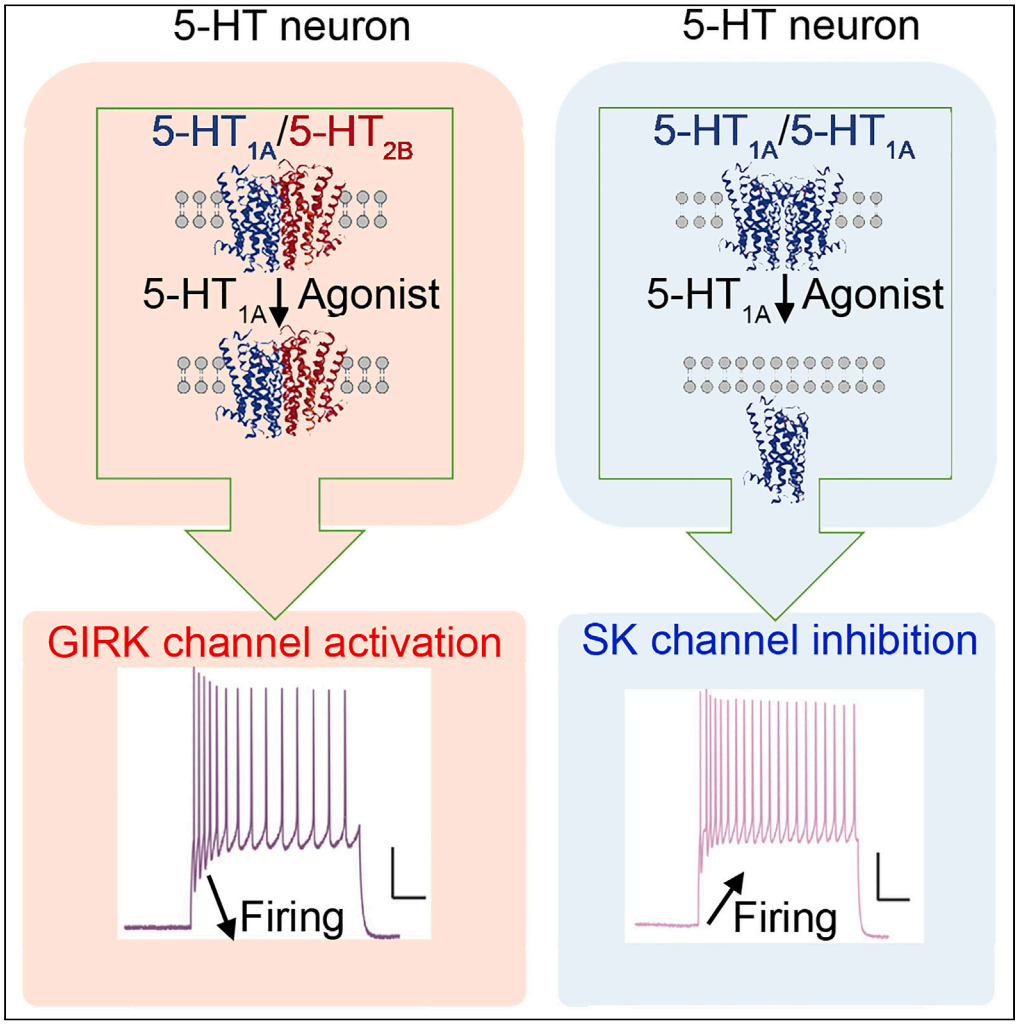

Amina Benhadda, Célia Delhaye, Imane Moutkine, ..., Anne Roumier, Sabine Lévi, Luc Maroteaux

luc.maroteaux@upmc.fr

Highlights

5-HT_{1A} and 5-HT_{2B} heterodimers co-cluster and are differentially regulated by agonist

With 5-HT_{2B}, 5-HT_{1A} activation decreases 5-HT neuron firing via GIRK channels

Without 5-HT_{2B}, 5-HT_{1A} activation increases 5-HT neuron firing via SK channels

5-HT_{1A}/5-HT_{2B} ratio tunes 5-HT neurons excitability that conditions SSRI efficacy

Benhadda et al., iScience *26*, 107401
August 18, 2023
https://doi.org/10.1016/j.isci.2023.107401

iScience

CellPress
OPEN ACCESS

Article

5-HT_{1A} and 5-HT_{2B} receptor interaction and co-clustering regulate serotonergic neuron excitability

Amina Benhadda,[1] Célia Delhaye,[1] Imane Moutkine,[1] Xavier Marques,[1] Marion Russeau,[1] Corentin Le Magueresse,[1] Anne Roumier,[1] Sabine Lévi,[1] and Luc Maroteaux[1,2,*]

SUMMARY

Many psychiatric diseases have been associated with serotonin (5-HT) neuron dysfunction. The firing of 5-HT neurons is known to be under 5-HT_{1A} receptor-mediated autoinhibition, but functional consequences of coexpressed receptors are unknown. Using co-immunoprecipitation, BRET, confocal, and super-resolution microscopy in hippocampal and 5-HT neurons, we present evidence that 5-HT_{1A} and 5-HT_{2B} receptors can form heterodimers and co-cluster at the plasma membrane of dendrites. Selective agonist stimulation of coexpressed 5-HT_{1A} and 5-HT_{2B} receptors prevents 5-HT_{1A} receptor internalization and increases 5-HT_{2B} receptor membrane clustering. Current clamp recordings of 5-HT neurons revealed that 5-HT_{1A} receptor stimulation of acute slices from mice lacking 5-HT_{2B} receptors in 5-HT neurons increased their firing activity trough Ca^{2+}-activated potassium channel inhibition compared to 5-HT neurons from control mice. This work supports the hypothesis that the relative expression of 5-HT_{1A} and 5-HT_{2B} receptors tunes the neuronal excitability of serotonergic neurons through potassium channel regulation.

INTRODUCTION

Many psychiatric diseases including depression, schizophrenia, or anxiety have been associated with serotonin (5-HT) neuron activity dysfunctions.[1–3] Dorsal raphe serotonin neurons (DR) and their long-range projections exert control over many physiological functions such as emotion, sleep, and locomotion. Pacemaker-like firing of raphe 5-HT neurons was reported to be under 5-HT_{1A} receptor (5-HT_{1A})-mediated autoinhibition, although 5-HT neurons can also express other 5-HT receptors. With the exception of 5-HT_3 receptors, which are ion channels, all 5-HT receptors are G-protein coupled receptors (GPCR) that differ according to their G-protein coupling.

The 5-HT_1 subtypes are typically coupled to the Gαi/o protein and their activation may lead to a decrease in intracellular cAMP level[4] among many other possible coupling depending on the cellular context.[5] In the central nervous system, 5-HT_{1A} functions as an autoreceptor, i.e., is expressed by 5-HT neurons themselves, in the raphe nuclei, and as heteroreceptors in neurons of several brain structures including hippocampus and prefrontal cortex.[5–7] In 5-HT neurons, 5-HT_{1A} are located to the somatodendritic compartment.[8] Through the Gβγ subunit, 5-HT_{1A} activation can induce the opening of potassium channels (G protein-coupled inwardly-rectifying potassium channels or GIRKs) which tends to hyperpolarize neurons.[9–12] The tone of 5-HT neurons has thus been considered to be negatively regulated by 5-HT_{1A} autoreceptors expressed on their soma and dendrites in the raphe nuclei.[11] Most serotonergic neurons have two key electrophysiological characteristics: a long-duration action potential and a prominent medium-duration afterhyperpolarization (mAHP), which plays a critical role in setting the firing frequency by delaying the occurrence of the next action potential.[13] This mAHP is due to the opening of small-conductance Ca^{2+}-activated potassium (SK) channels. Blockade of SK channels by apamin, a neurotoxin from bee venom, which is a potent antagonist of SK2 and SK3 subtypes, has been shown to increase 5-HT neuron burst firing (repeated action potentials separated by a small interval) in DR and extracellular 5-HT levels[14] via a direct action.[15] It has been proposed that 5-HT_{1A} may also regulate SK channels,[16] in addition to GIRKs. Accumulating evidence indicate additional roles for 5-HT_{1A} in dorsal raphe beyond an homeostatic control of firing rate.[6] In particular, the 5-HT_{1A} autoreceptors internalization, which results in its desensitization[17] is thought to participate to the delayed antidepressant effects

[1]Institut du Fer à Moulin, U1270 INSERM, Sorbonne Université, 17 rue du Fer à Moulin, 75005 Paris, France

[2]Lead contact

*Correspondence: luc.maroteaux@upmc.fr

https://doi.org/10.1016/j.isci.2023.107401

of serotonin-specific reuptake inhibitors (SSRIs). Nevertheless, there is evidence that 5-HT_{1A}-dependent feedback inhibition of 5-HT neurons persists after sustained chronic exposure to high extracellular 5-HT as upon exposure to SSRIs.[18] Therefore, we asked if 5-HT_{1A} could interact with other 5-HT receptors to participate to the regulation of 5-HT neuron firing.

The 5-HT_2 receptor subtypes (5-$HT_{2A, 2B, 2C}$) are coupled to the Gαq/11 protein that mainly activate phospholipase C (PLC) and increase inositol triphosphate (IP3) and Ca^{2+} intracellular concentration. A loss of function of *HTR2B*, the gene encoding 5-HT_{2B}, is associated with impulsivity, a higher risk of developing depression and suicidal behavior.[19,20] Using behavioral and biochemical experiments in mice, Diaz et al.[21] showed that 5-HT_{2B} is expressed in serotonergic neurons, which is confirmed by recent RNAseq[22,23] (see https://bokaty.shinyapps.io/DR_Pet1_neuron_scRNAseq_DB/). The acute or chronic activation of 5-HT_{2B} by the preferential agonist BW723C86 (BW) can mimic SSRI effects in mice.[21] Accordingly, behavioral and molecular responses to SSRIs are abolished in mice lacking the 5-HT_{2B} specifically in 5-HT neurons (2B-KO^{5-HT} mice). Moreover, in WT mice, the activation of 5-HT_{2B} by BW is able to counteract the effects of 5-HT_{1A} autoreceptor activation by the selective agonist 8-hydroxy-2-(di-*n*-propylamino)tetralin (8-OHDPAT), such as the decrease in 5-HT neurons firing rate and in body temperature.[24] Although 5-HT_2 signaling has been shown to crosstalk with 5-HT_{1A},[25] and 5-HT_{2B} are expressed by serotonergic neurons together with 5-HT_{1A},[21] interactions between these receptors and their putative consequence to serotonergic tone regulation are not yet documented.

The aim of this work was thus to test the hypothesis that interactions between 5-HT_{2B} and 5-HT_{1A} affect their impact on 5-HT neurons activity. By studying different models (COS-7 cells, primary cultures of hippocampal neurons, and raphe 5-HT neurons) with pharmacological, electrophysiological, and high-resolution imaging techniques, we show that 5-HT_{2B} and 5-HT_{1A} can form heterodimers. Moreover, coexpression of both receptors has no apparent effect on their respective ligand binding properties and their classical second messenger signaling, but alters their plasma membrane expression (local accumulation as clusters, cell membrane expression) during responses to specific ligands. Last, *ex vivo* experiments reveal that their crosstalk affects the excitability of 5-HT neurons through SK and GIRK channels regulation.

RESULTS

Coexpression of 5-HT_{2B} with 5-HT_{1A} reveals direct interactions

We previously showed that 5-HT_{2B} and 5-HT_{1A} can be coexpressed in 5-HT neurons[21] and have opposite actions on 5-HT neuronal activity.[24] GPCRs including 5-HT receptors are able to form homo or heterodimers with each other or with non-5-HT receptors that modify their respective signaling pathways.[26] To assess putative 5-HT_{2B} and 5-HT_{1A} interactions, we first performed co-immunoprecipitation experiments in COS-7 cells transfected with plasmids encoding HA-tagged 5-HT_{2B} and/or Myc-tagged 5-HT_{1A} (See STAR methods). Immunoprecipitation of 5-HT_{2B} with anti-HA beads followed by Western blotting with anti-Myc antibody to assess the presence of 5-HT_{1A} revealed co-immunoprecipitation of 5-HT_{1A} with 5-HT_{2B} in cotransfected cells (Figure 1A). We completed these data by performing BRET experiments to assess close vicinity of 5-HT_{1A} and 5-HT_{2B}. This experiment relies on the natural capacity of Renilla luciferase, used here as BRET donor, to emit energy in presence of its substrate, coelenterazine or to transfer it to an acceptor. The sequences of Luciferase (the BRET donor) and of yellow fluorescent protein (YFP, the BRET acceptor) were fused to the C-terminal coding region of 5-HT_{1A} and 5-HT_{2B}, respectively (See STAR methods). Increasing amounts of BRET acceptor plasmids were co-transfected with a constant amount of BRET donor plasmid in COS-7 cells. A hyperbolic curve indicates saturation and thus specific interaction between the BRET donor and the acceptor and thus, the close proximity between the two proteins that carry them. Here, a hyperbolic curve was obtained when 5-HT_{2B} and 5-HT_{1A} were expressed together, supporting the hypothesis that they can form heterodimers in intact cells (Figure 1B). As control, no BRET signal was obtained when 5-HT_{2B} was tested for self-association, confirming a previous study indicating that this receptor is unable to form homodimers.[27] Thus, co-immunoprecipitation and BRET experiments revealed that 5-HT_{1A} and 5-HT_{2B} can interact closely and may form heteromers.

Total receptor expression and coupling to second messenger are not affected by 5-HT_{2B}/5-HT_{1A} coexpression

We assessed if coexpression of 5-HT_{1A} and 5-HT_{2B} affect their respective intracellular signaling pathway, and pharmacological properties. To this aim, we transfected COS-7 cells to express 5-HT_{2B} and/or 5-HT_{1A}, either alone or together, and prepared whole membrane protein extracts. We then performed radioligand binding competition assays for 5-HT_{2B} and 5-HT_{1A} in the different transfection conditions, to assess their Bmax, which

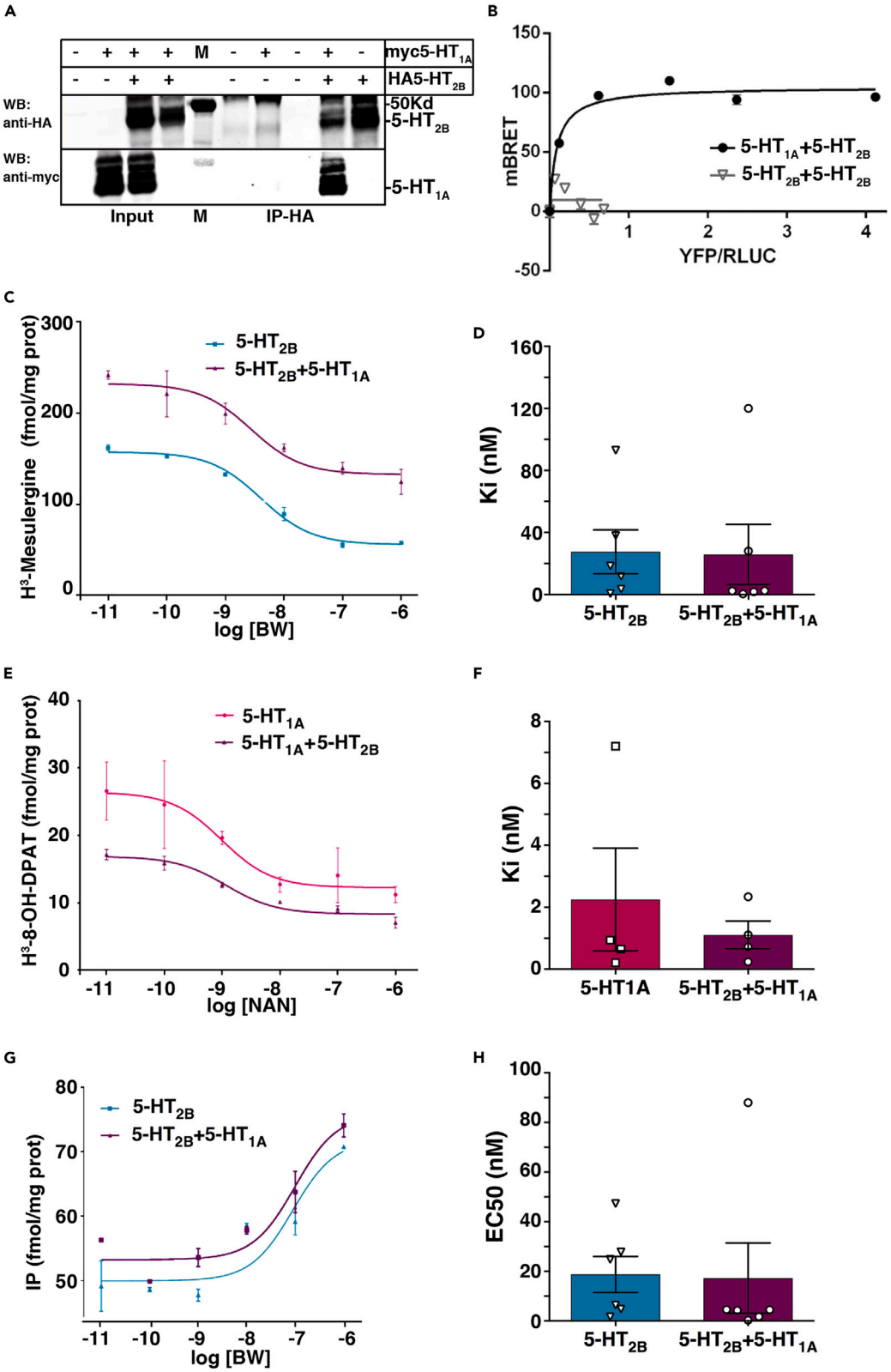
A
myc5-HT1A
HA5-HT2B
WB: anti-HA
WB: anti-myc
50Kd
5-HT2B
5-HT1A
Input
M
IP-HA
B
mBRET
YFP/RLUC
5-HT1A+5-HT2B
5-HT2B+5-HT2B
C
H3-Mesulergine (fmol/mg prot)
log [BW]
5-HT2B
5-HT2B+5-HT1A
D
Ki (nM)
5-HT2B
5-HT2B+5-HT1A
E
H3-8-OH-DPAT (fmol/mg prot)
log [NAN]
5-HT1A
5-HT1A+5-HT2B
F
Ki (nM)
5-HT1A
5-HT2B+5-HT1A
G
IP (fmol/mg prot)
log [BW]
5-HT2B
5-HT2B+5-HT1A
H
EC50 (nM)
5-HT2B
5-HT2B+5-HT1A

Figure 1. Physical proximity of 5-HT$_{2B}$ and 5-HT$_{1A}$ in transfected cells does not affect second messenger signaling

(A) Co-immunoprecipitation of 5-HT$_{1A}$ with 5-HT$_{2B}$ in COS-7 cells. Proteins from COS-7 cells co-transfected with plasmids coding for HA-tagged 5-HT$_{2B}$ (HA-5-HT$_{2B}$) and myc-tagged 5-HT$_{1A}$ (myc-5-HT$_{1A}$) were immunoprecipitated with an anti-HA antibody and analyzed by anti-HA (top) or anti-myc (bottom) Western-blotting. Western-blots on the whole extract ("input") show the presence of the receptors in each condition (Input; left panel). Immunoprecipitations using anti-HA beads (IP-HA; right panel) reveal a co-immunoprecipitation between 5-HT$_{1A}$ and 5-HT$_{2B}$. Molecular weight marker of 50 Kd (M).

(B) BRET proximity assays for 5-HT$_{1A}$ and 5-HT$_{2B}$. COS-7 cells were co-transfected with a constant amount of plasmid coding for 5-HT$_{2B}$-RLuc (BRET donor) and increasing amounts of plasmid encoding YFP-tagged 5-HT$_{1A}$ (5-HT$_{1A}$-YFP BRET acceptor) or YFP-tagged 5-HT$_{2B}$ (5-HT$_{2B}$-YFP) as negative control unable to form dimers.[27] The hyperbolic curve attests close interaction between 5-HT$_{1A}$-YFP and 5-HT$_{2B}$-RLuc with a physical distance <10 nm (representative experiment of n > 3 independent experiments).

(C–H) Pharmacological characterization of co-expressed receptors. Radioligand binding competition by BW or NAN of tritiated-mesulergine (C and D) or 8-OH-DPAT (E and F) performed on whole membrane proteins from transfected COS-7 cells expressing 5-HT$_{2B}$ with or without 5-HT$_{1A}$. Coexpression of 5-HT$_{2B}$ with 5-HT$_{1A}$ did not modify the binding affinity to their respective ligand (Ki) compared to single 5-HT$_{2B}$ expression. Data were analyzed using the Mann-Whitney unpaired t-test. Representative curves of n = 3 independent experiments, each performed in duplicate. (G and H) Impact of coexpression on 5-HT$_{2B}$- and 5-HT$_{1A}$-operated signal transduction. The quantification of inositol phosphate was performed in COS-7 cells expressing 5-HT$_{2B}$ with or without 5-HT$_{1A}$ and stimulated with increasing concentrations of the 5-HT$_{2B}$ agonist BW. Note the absence of effect, in the coexpression of 5-HT$_{2B}$ with 5-HT$_{1A}$, on IP production compared to the single 5-HT$_{2B}$ expression condition. Data were statistically analyzed by Mann-Whitney unpaired t-test. Representative curves of n = 3 independent experiments, each performed in duplicate. Individual values are presented with mean ± SEM.

represents the total number of receptors available, and their Ki, which represents the affinity, for their specific ligand (See STAR methods). No difference was found in Bmax (not illustrated), nor in binding affinity (Ki) to their respective ligand, in coexpressing compared to single receptor expressing cells (Figures 1C–1F). The Ki of 5-HT$_{2B}$ for its specific ligand BW was not affected by the coexpression of 5-HT$_{1A}$ (Figure 1D). Similarly, the Ki of 5-HT$_{1A}$ for its specific ligand NAN was not affected by the coexpression of 5-HT$_{2B}$ (Figure 1F). This indicates that even if 5-HT$_{1A}$ and 5-HT$_{2B}$ can form heterodimers, as indicated by coIP and BRET experiments, this doesn't significantly change their affinity for ligands. Then, using HTRF-based assays, we measured the intracellular inositol phosphate (IP) amount produced by agonist stimulation of 5-HT$_{2B}$, in cells expressing both 5-HT$_{2B}$ and 5-HT$_{1A}$ or 5-HT$_{2B}$ alone. IP measurement is a readout of the activation of Gq/PLC/IP3 pathway, which is the classical downstream signaling of 5-HT$_{2B}$ (See STAR methods). The dose-response curve of IP production in response to increasing doses of BW, a specific agonist of 5-HT$_{2B}$, were analyzed using the operational model to determine the Gαq coupling efficiency of the receptor either alone or expressed together with 5-HT$_{1A}$. This showed that there was no significant difference in the EC50 between the two conditions (Figures 1G and 1H). These results indicate that 5-HT$_{1A}$ and 5-HT$_{2B}$ coexpression modifies neither their total expression level, nor their ligand binding, nor the Gαq/11 coupling efficiency of 5-HT$_{2B}$.

Coexpression of 5-HT$_{2B}$ with 5-HT$_{1A}$ decreases 5-HT$_{2B}$ membrane expression

Trafficking of GPCRs to the plasma membrane is a process which can be regulated, notably by the expression and/or stimulation of other GPCRs.[26] In the absence of modification of the total expression level nor coupling properties of 5-HT$_{2B}$ when coexpressed with 5-HT$_{1A}$, we investigated putative changes in their expression at the plasma membrane. First, we evaluated 5-HT$_{2B}$ density at the plasma membrane using again radioligand binding competition assays, this time on living, non-permeabilized, cells (See STAR methods). Here, we observed that coexpression of the two receptors did not modify the 5-HT$_{2B}$ Ki but significantly decreased its Bmax, i.e., the amount of 5-HT$_{2B}$ present at the plasma membrane. Bmax for 5-HT$_{2B}$ was indeed 60% lower when this receptor was expressed together with 5-HT$_{1A}$ than when expressed alone (Figures 2A and 2B). In contrast, 5-HT$_{1A}$ plasma membrane expression levels were similar with and without coexpression of 5-HT$_{2B}$ (not illustrated). To confirm these results, we performed biotinylation assay, and evaluated the ratio of the membrane/total protein expression level for each receptor (See STAR methods). This showed that coexpression of the two receptors significantly decreased, by 31%, the amount of 5-HT$_{2B}$ reaching the membrane (Figures 2C and 2D), but did not impact 5-HT$_{1A}$ membrane expression (Figures 2C–2E). Together, these data indicate that the 5-HT$_{2B}$ membrane expression is reduced by coexpression of 5-HT$_{1A}$.

Neuronal co-distribution of 5-HT$_{1A}$ and 5-HT$_{2B}$ in somatodendritic compartment

Membrane proteins, including GPCRs, are targeted to specialized membrane domains, or clusters, via interactions with scaffolding proteins that are not only important for the regulation of synaptic transmission

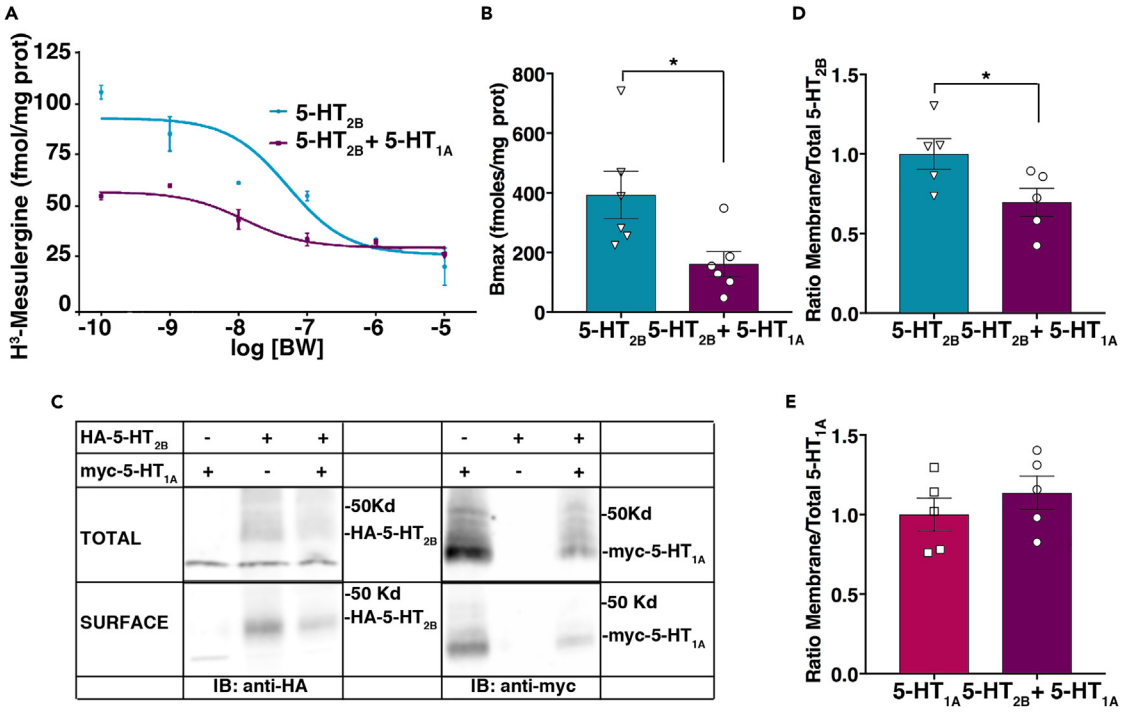

Figure 2. 5-HT$_{2B}$/5-HT$_{1A}$ co-expression decreases 5-HT$_{2B}$ plasma membrane expression

(A) Radioligand binding competition by BW of tritiated mesulergine performed on membrane proteins of intact (non-permeabilized) COS-7 cells transfected to express 5-HT$_{2B}$ alone or with 5-HT$_{1A}$.

(B) Co-expression decreases membrane expression of 5-HT$_{2B}$, as illustrated by a significant decrease in Bmax ($p = 0.0336$). Data were analyzed using unpaired t-test with Welch's correction; n = 3 independent experiments, each performed in duplicate.

(C–E) Surface biotinylation performed on COS-7 cells expressing 5-HT$_{1A}$ and/or 5-HT$_{2B}$. (C) Analysis by Western blotting. (D and E) Ratio of the membrane/total protein levels for each receptor analyzed in conditions of simple or co-expression. Co-expression of the two receptors limits the proportion of 5-HT$_{2B}$ (unpaired t-test $p = 0.0477$, n = 5) but not 5-HT$_{1A}$ (unpaired t-test $p = 0.3834$, n = 5) reaching the plasma membrane. Representative curves of n = 5 independent experiments. Band intensity of each condition was quantified and represented graphically. (*$p < 0,05$). Individual values are presented with mean ± SEM.

but also for the formation of signaling complexes. Receptor clustering controls signaling, trafficking, and cytoskeletal rearrangements around synapses.[28] We previously showed that 5-HT$_{2B}$ is localized in the somatodendritic compartment of transfected hippocampal cultured neurons and form clusters which reflect local accumulation of receptors.[29] 5-HT$_{2B}$ can positively regulate the activity of 5-HT neurons, in a manner opposite to 5-HT$_{1A}$.[24] Independently, 5-HT$_{1A}$ were shown to be expressed in the somatodendritic compartment of 5-HT and hippocampal neurons *in vivo*[30,31] and in cultures.[32] However, to date, the lack of selective and sensitive antibodies against these two receptors makes studies on endogenous receptors impossible. To assess their relative subcellular distribution, we thus transfected hippocampal neurons in cultures with plasmids encoding HA-tagged-5-HT$_{2B}$ and myc-tagged-5-HT$_{1A}$ (See STAR methods). Both 5-HT$_{1A}$ and 5-HT$_{2B}$ located in the somatodendritic compartment, consistently with previous reports, but they displayed different distribution patterns: at the membrane of dendrites, 5-HT$_{2B}$ were arranged in large clusters, whereas 5-HT$_{1A}$ formed much smaller clusters, some of which are colocalized with 5-HT$_{2B}$ clusters (Figure 3A). We also observed, in these cultures of hippocampal neurons, that coexpression of 5-HT$_{1A}$ decreased by 28% the membrane/total ratio of 5-HT$_{2B}$ (Figure 3B), confirming the effect previously observed in COS-7 cells (Figure 2). Together, these data indicate that 5-HT$_{2B}$ and 5-HT$_{1A}$ are addressed to the somatodendritic compartment in neuron in culture, and may functionally interact.

Upon coexpression, selective stimulation of either 5-HT$_{1A}$ or 5-HT$_{2B}$ increases 5-HT$_{2B}$ membrane clustering and maintains expression of 5-HT$_{1A}$ at the plasma membrane

In transfected COS-7 cells and cultured hippocampal neurons, we observed that the addressing of 5-HT$_{2B}$ to the plasma membrane was altered by coexpression of 5-HT$_{1A}$. Importantly, another parameter that can affect receptor function is its membrane clustering.[33] Moreover, this distribution can be modified upon

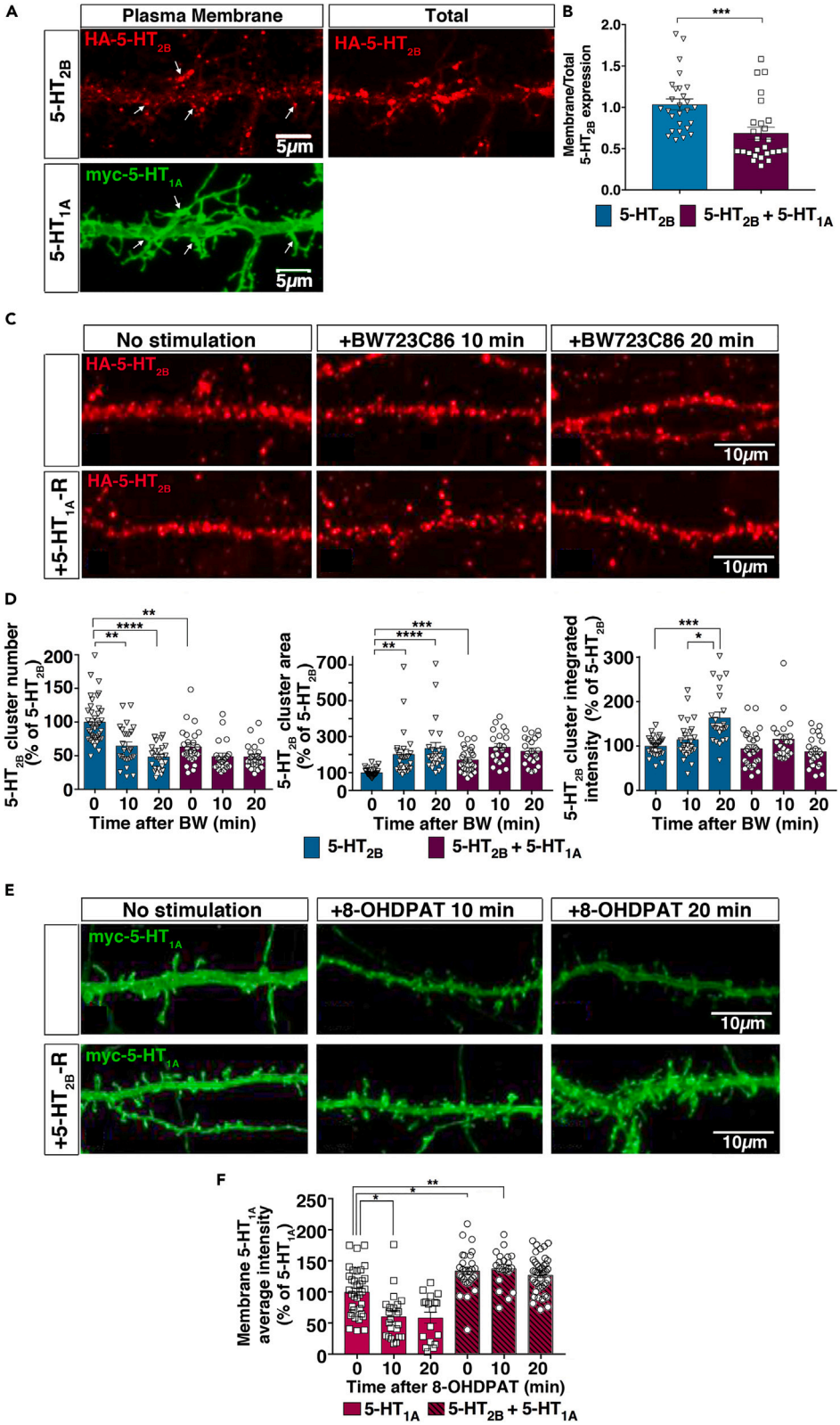
A
Plasma Membrane
Total
5-HT2B
HA-5-HT2B
5μm
5-HT1A
myc-5-HT1A
5μm
B
***
Membrane/Total 5-HT2B expression
2.0
1.5
1.0
0.5
0.0
5-HT2B
5-HT2B + 5-HT1A
C
No stimulation
+BW723C86 10 min
+BW723C86 20 min
HA-5-HT2B
10μm
+5-HT1A-R
HA-5-HT2B
10μm
D
5-HT2B cluster number (% of 5-HT2B)
5-HT2B cluster area (% of 5-HT2B)
5-HT2B cluster integrated intensity (% of 5-HT2B)
Time after BW (min)
0 10 20 0 10 20
5-HT2B
5-HT2B + 5-HT1A
E
No stimulation
+8-OHDPAT 10 min
+8-OHDPAT 20 min
myc-5-HT1A
10μm
+5-HT2B-R
myc-5-HT1A
10μm
F
Membrane 5-HT1A average intensity (% of 5-HT1A)
Time after 8-OHDPAT (min)
0 10 20 0 10 20
5-HT1A
5-HT2B + 5-HT1A

Figure 3. Co-expression of 5-HT$_{2B}$ with 5-HT$_{1A}$ in hippocampal neurons increases 5-HT$_{2B}$ membrane clustering and maintains 5-HT$_{1A}$ surface expression upon selective agonist stimulation

(A) 5-HT$_{2B}$ localization by HA-tag immunostaining (red) revealed receptor clustering at the dendritic membrane of hippocampal neurons, whereas 5-HT$_{1A}$ localization studied by myc-tag immunostaining (green) revealed a more even distribution in smaller clusters, which are in part colocalized with 5-HT$_{2B}$ clusters (white arrows).

(B) Quantification of the staining intensities in the absence (plasma membrane expression) or in the presence (total expression) of detergent indicates that co-expressing 5-HT$_{1A}$ with 5-HT$_{2B}$ decreases the membrane/total ratio of 5-HT$_{2B}$ (values normalized to the ratio in 5-HT$_{2B}$ single transfection condition, $p = 0.0084$, as assessed by unpaired t-test; n = 20–24 dendrites from 3 independent cell cultures; Scale bars, 5 μm).

(C) 5-HT$_{2B}$ clustering at the dendritic membrane 0, 10 or 20 min after BW stimulation in the absence (top) or presence (bottom) of 5-HT$_{1A}$. Scale bars, 10 μm.

(D) Quantification of 5-HT$_{2B}$ membrane clustering following agonist stimulation in the presence (or not) of 5-HT$_{1A}$. Upon 5-HT$_{2B}$ stimulation by BW (1 μM), the number of 5-HT$_{2B}$ clusters decreased in the absence of 5-HT$_{1A}$ ($p = 0.0026$ t0 vs. t10 and $p < 0.0001$ t0 vs. t20), as revealed by Kruskal-Wallis test, $p < 0.0001$, followed by Dunn's multiple comparisons test; in the presence of 5-HT$_{1A}$, the 5-HT$_{2B}$ cluster number decreased in the absence of BW stimulation and was unaffected by BW stimulation, $p = 0.004$ t0 5-HT$_{2B}$ vs. t0 5-HT$_{1A}$. The BW stimulation of 5-HT$_{2B}$ alone increased the cluster size (area), $p = 0.0016$ t0 vs. t10 and $p < 0.0001$ t0 vs. t20; in the presence of 5-HT$_{1A}$, the 5-HT$_{2B}$ cluster area increased but was unaffected by BW stimulation, $p = 0.0008$ t0 5-HT$_{2B}$ vs. t0 5-HT$_{1A}$. The BW stimulation slightly increased the molecular density of clusters (integrated intensity) of 5-HT$_{2B}$ clusters from 0 to 20 min in the absence of 5-HT$_{1A}$, $p = 0.00007$ t0 vs. t20; in the presence of 5-HT$_{1A}$, the 5-HT$_{2B}$ cluster integrated intensity was unaffected without or with BW stimulation. n = 19–38 dendrites from 3 to 4 independent cell cultures.

(E) 5-HT$_{1A}$ expression at the dendritic membrane 0, 10 or 20 min after 8-OH-DPAT stimulation in the absence (top) or presence (bottom) of 5-HT$_{2B}$. Scale bars, 10 μm.

(F) Quantification of 5-HT$_{1A}$ membrane expression following agonist stimulation in the presence (or not) of 5-HT$_{2B}$. Upon 5-HT$_{1A}$ stimulation by 8-OH-DPAT (1 μM), 5-HT$_{1A}$ expression at the neuronal membrane decreased from 0 to 10 min in the absence of 5-HT$_{2B}$ compared to t0 as revealed by Kruskal-Wallis test, $p < 0.0001$, followed by Dunn's multiple comparisons test, $p = 0.0115$ t0 vs. t10; in the presence of 5-HT$_{2B}$, the 5-HT$_{1A}$ expression increased but was unaffected by 8-OH-DPAT stimulation, $p = 0.0172$ t0 5-HT$_{2B}$ vs. t0 5-HT$_{1A}$+5-HT$_{2B}$. n = 18–43 dendrites from 3 independent cell cultures. In all graphs, data, expressed as percentage of their respective values at t0. ****$p < 0.0001$, ***$p < 0.001$, **$p < 0.01$, *$p < 0.05$. Individual values are presented with mean ± SEM.

receptor stimulation, which will subsequently alter their function. We thus studied by confocal microscopy the distribution of 5-HT$_{2B}$ and 5-HT$_{1A}$ expressed alone or together, at the plasma membrane of cultured hippocampal neurons, in basal condition and after stimulation of one receptor or the other. Selective agonists of each receptor were selected in order to limit possible cross-activation: the 5-HT$_{1A}$ selective agonist 8-OHDPAT, which displays 1 nM affinity for 5-HT$_{1A}$ and 5 μM affinity for 5-HT$_{2B}$ and the preferential 5-HT$_{2B}$ agonist BW723C86, which has 10 nM affinity for 5-HT$_{2B}$, over 1 μM for 5-HT$_{1A}$, and over 10-fold lower affinity for other 5-HT$_2$ receptors (see PDSP database https://pdsp.unc.edu/databases/pdsp.php). We first quantified the number and size of 5-HT$_{2B}$ clusters and their integrated intensity, which reflects the density of receptors per cluster. We observed that when 5-HT$_{2B}$ was expressed alone, its stimulation with the specific agonist BW (1μM) for 20 min decreased the number of 5-HT$_{2B}$ clusters (−51%) but increased their size (+97%) and intensity (+64%) (Figures 3C and 3D). Interestingly, expression of 5-HT$_{1A}$, even in the absence of any stimulation, was sufficient to induce quite similar effects, i.e., to decrease the number of 5-HT$_{2B}$ clusters (−36%) and to increase their area (+73%), but with no significant effect on their density (Figures 3C and 3D). Selective stimulation by BW of the cotransfected neurons did not further significantly change these parameters.

Then, we quantified the plasma membrane expression level of 5-HT$_{1A}$. Selective stimulation of 5-HT$_{1A}$ by 8-OH-DPAT (1 μM) led to a reduction of 5-HT$_{1A}$ expression at the plasma membrane, as shown by the decrease in membrane 5-HT$_{1A}$ fluorescence intensity over time (−41%), which suggests an internalization of the receptors (Figures 3E and 3F). In contrast, coexpression of 5-HT$_{2B}$ resulted in a +34% increase in 5-HT$_{1A}$ expression at the plasma membrane, even in basal, non-stimulated condition, and prevented the decrease of membrane 5-HT$_{1A}$ upon 8-OH-DPAT stimulation (Figures 3E and 3F). Altogether, these results indicate that the coexpression of 5-HT$_{2B}$ and 5-HT$_{1A}$ increases the clustering (lower number, but bigger size of clusters) of 5-HT$_{2B}$ and the membrane expression of 5-HT$_{1A}$, and prevents the effects of receptors agonists on their subcellular distribution, confirming a functional interaction between 5-HT$_{2B}$ and 5-HT$_{1A}$.

Clusters of receptors are small objects, and the 200-nm diffraction limit of confocal microscopy does not allow isolation of nearby clusters (Figure 4A). Using Stochastic Optical Reconstruction Microscopy

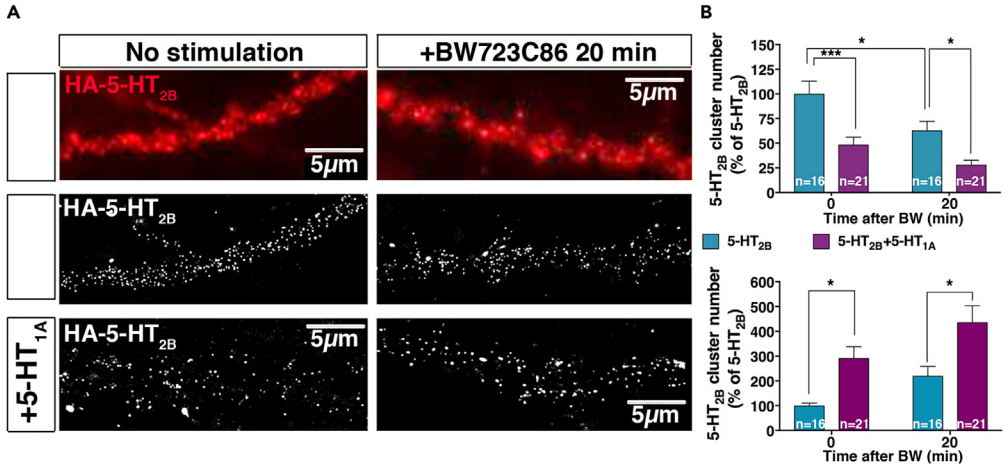

Figure 4. Super-resolution microscopy fully validates that co-expression of 5-HT$_{2B}$ with 5-HT$_{1A}$ increases 5-HT$_{2B}$ membrane clustering as upon BW agonist stimulation

(A) (Top) Images of 5-HT$_{2B}$ membrane clusters acquired by epifluorescence microscopy. Note that clusters are not well-defined and diffuse compared to the lower images acquired at super resolution. Scale bar, 5 µm. (Middle and Bottom). STORM images of 5-HT$_{2B}$ obtained from the dendritic regions shown in A before (left panel) or 20 min (right panel) after BW stimulation in the absence (middle) or presence (bottom) of 5-HT$_{1A}$. Scale bars, 5 µm.

(B) Quantification of 5-HT$_{2B}$ clustering following agonist stimulation in the presence or not of 5-HT$_{1A}$. The number of 5-HT$_{2B}$ clusters was significantly decreased upon stimulation by BW (1 µM) or by co-expression with 5-HT$_{1A}$. two-way ANOVA revealed main effects of agonist treatment $F_{1,\ 70} = 11.15$, $p = 0.0014$ and receptor expression $F_{1,\ 70} = 25.31$, $p < 0.0001$; t0 5-HT$_{2B}$ vs. t0 5-HT$_{2B}$+5-HT$_{1A}$ $p = 0.0004$; t20 5-HT$_{2B}$ vs. t20 5-HT$_{2B}$+5-HT$_{1A}$ $p = 0.028$; t0 vs. t20 5-HT$_{2B}$, $p = 0.0271$ by Tukey's multiple comparisons test. The area of 5-HT$_{2B}$ clusters was significantly increased upon stimulation by BW for 20 min (t20) or by co-expression with 5-HT$_{1A}$. two-way ANOVA revealed main effects of agonist treatment $F_{1,\ 70} = 7.067$, $p = 0.0097$ and receptor expression $F_{1,\ 70} = 16.78$, $p = 0.0001$; t0 5-HT$_{2B}$ vs. t0 5-HT$_{2B}$+5-HT$_{1A}$ $p = 0.0402$; t20 5-HT$_{2B}$ vs. t20 5-HT$_{2B}$+5-HT$_{1A}$ $p = 0.0156$ by Tukey's multiple comparisons test. n = 16–21 dendrites from 3 independent cell cultures. Data are expressed as percentage of their respective values at t0. ****$p < 0.0001$, ***$p < 0.001$, **$p < 0.01$, *$p < 0.05$. Bars and error bars represent mean ± SEM.

(STORM) technique with a resolution up to 20 nm, we confirmed our initial observation (See STAR methods): coexpression of 5-HT$_{1A}$ with 5-HT$_{2B}$, with or without 5-HT$_{2B}$ stimulation by BW, significantly decreased the number of 5-HT$_{2B}$ cluster (−52% and −55%, respectively) and increased their area (+292% and +150%, respectively) (Figure 4B). Thanks to its better resolution compared to confocal microscopy, this technique revealed in addition a significant potentiation by BW stimulation (two-fold) of the effects of 5-HT$_{1A}$ coexpression on 5-HT$_{2B}$ clustering (decrease in number and increase in area) (Figure 4B). Together, these results confirmed that the coexpression of 5-HT$_{1A}$ mimics some of the effects of 5-HT$_{2B}$ stimulation by BW on its membrane distribution.

Selective stimulation of either 5-HT$_{1A}$ or 5-HT$_{2B}$ generates crossed effects on the other receptor's distribution at the plasma membrane

Since coexpression of both receptors was preventing most of the effect of the orthologous stimulation of either receptor, we asked whether stimulating one receptor would differentially impact the other receptor in cotransfected neurons. In coexpression condition, 5-HT$_{1A}$ membrane expression was increased (+28%) compared to the single expression condition, as expected, but when we stimulated these cells with the selective 5-HT$_{2B}$ agonist BW for 20 min, we reversed this increase and even induced a decrease (−28%) in 5-HT$_{1A}$ membrane expression compared to the unstimulated condition (Figures 5A and 5B). Conversely, in neurons expressing both 5-HT$_{1A}$ and 5-HT$_{2B}$, and stimulated with the selective 5-HT$_{1A}$ agonist 8-OH-DPAT for 20 min, we observed a decrease (−49%) in the number of 5-HT$_{2B}$ cluster, together with an increase in their size (+99%) and intensity (+89%) (Figures 5C–5F). Thus, the stimulation of 5-HT$_{1A}$ by its agonist enhances the effects of 5-HT$_{1A}$ coexpression on 5-HT$_{2B}$ clustering (i.e., induction of less but bigger and brighter clusters) reported in Figures 3C and 3D. These data suggest a cooperative association between 5-HT$_{2B}$ and 5-HT$_{1A}$ at the membrane of neurons, with 5-HT$_{1A}$ stimulation increasing 5-HT$_{2B}$ clustering and 5-HT$_{2B}$ stimulation decreasing 5-HT$_{1A}$ membrane expression.

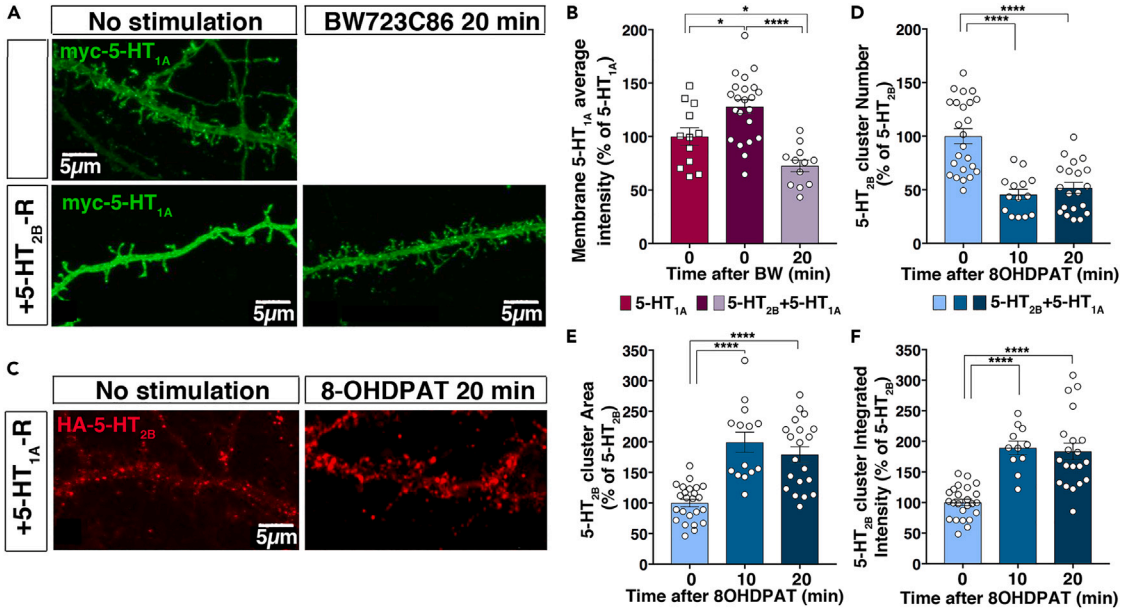

Figure 5. Cross-stimulation of 5-HT$_{2B}$ or 5-HT$_{1A}$ affects their respective membrane expression

(A) Images of 5-HT$_{1A}$ membrane expression acquired by confocal microscopy. 5-HT$_{1A}$ (green) in the absence (top) or presence of 5-HT$_{2B}$, (bottom) before or 20 min after BW stimulation. Scale bar, 10 μm.

(B) Quantification of 5-HT$_{1A}$ membrane expression in neurons expressing 5-HT$_{1A}$ alone or in combination with 5-HT$_{2B}$, with or without 5-HT$_{2B}$ stimulation by BW (1 μM). One-way ANOVA analysis shows a significant effect of the co-expression of 5-HT$_{2B}$ $F_{2,\ 43} = 16.15$, $p < 0.0001$, with an increase in 5-HT$_{1A}$ membrane expression, as shown by Tukey's multiple comparison ($p = 0.0188$ vs. non-stimulated 5-HT$_{1A}$); the 5-HT$_{2B}$ stimulation by BW in co-expression experiment abolishes this effect ($p < 0.0001$ vs. non-stimulated) and even reverses this effect ($p = 0.0463$) as compared to non-stimulated neurons expressing 5-HT$_{1A}$ alone. n = 12–22 dendrites from 2 independent cell cultures.

(C) Images of 5-HT$_{2B}$ membrane expression acquired by confocal microscopy. 5-HT$_{2B}$ (red) clustering at the dendritic membrane before or after 8-OH-DPAT stimulation (t20, 20 min) in the presence of 5-HT$_{1A}$. Scale bar, 10 μm.

(D–F) Quantification of 5-HT$_{2B}$ clustering in neurons co-expressing 5-HT$_{1A}$ in control condition or after 10 or 20 min of 5-HT$_{1A}$ stimulation with 8-OH-DPAT (1 μM). (D) Upon stimulation by 8-OH-DPAT, the number of 5-HT$_{2B}$ clusters decreased as revealed by Kruskal-Wallis test, $p < 0.0001$, followed by Dunn's multiple comparisons test; $p < 0.0001$ t0 vs. t10 and $p = 0.0001$ t0 vs. t20; (E) their area was increased, as revealed by Kruskal-Wallis test, $p < 0.0001$, followed by Dunn's multiple comparisons test, $p < 0.0001$, t0 vs. t10 and $p < 0.0001$ t0 vs. t20; (F) their molecular density (integrated intensity) was also increased, as revealed by Kruskal-Wallis test, $p < 0.0001$, followed by Dunn's multiple comparisons test, $p < 0.0001$ t0 vs. t10 and $p < 0.0001$ t0 vs. t20. Data are expressed as percentage of their respective values at t0. n = 11–24 dendrites from 3 independent cell cultures. ****$p < 0.0001$, ***$p < 0.001$, **$p < 0.01$, *$p < 0.05$. Individual values are presented with mean ± SEM.

Co-stimulation of both receptors by 5-HT suppresses 5-HT$_{2B}$ effect on 5-HT$_{1A}$ clustering

Since 5-HT$_{1A}$ and 5-HT$_{2B}$ respective agonists have different effects on the membrane clustering and localization of either receptor, we investigated the effect of co-stimulation with their natural ligand, 5-HT, on their distribution. Surprisingly, stimulation with 5-HT (1 μM) did not modify 5-HT$_{2B}$ cluster properties: neither the plasma membrane cluster density, nor the cluster size and intensity were affected by the coexpression of 5-HT$_{1A}$ (Figure 6A). On the contrary, stimulation with 5-HT decreased 5-HT$_{1A}$ membrane expression by −39% compared to unstimulated condition (Figures 6B and 6C), and close to what was observed after 8-OH-DPAT application (Figures 3E and 3F). When coexpressed with 5-HT$_{2B}$, 5-HT$_{1A}$ membrane expression increased by +24%, and 5-HT stimulation decreased this membrane expression by −50%, this effect being fully reversed by the selective 5-HT$_{2B}$ antagonist, RS (Figure 6C). This result supports the notion that stimulating both 5-HT$_{2B}$ and 5-HT$_{1A}$ by 5-HT reverses the 5-HT$_{2B}$ ability to maintain the 5-HT$_{1A}$ at the plasma membrane (Figure 6C). These data indicate a differential crosstalk between 5-HT$_{2B}$ and 5-HT$_{1A}$ according to agonist selectivity, 5-HT vs. 8-OH-DPAT or BW.

Colocalized 5-HT$_{2B}$/5-HT$_{1A}$ control the firing of 5-HT neurons by acting at apamin-sensitive SK channels

To study putative *in vivo* colocalization of 5-HT$_{2B}$ and 5-HT$_{1A}$ in 5-HT neurons, we stereotactically injected in the B7 raphe nuclei of *Pet1-Cre*$^{+/0}$ mice pAAV-EF1A-DIO-WPRE-pA viruses to specifically express

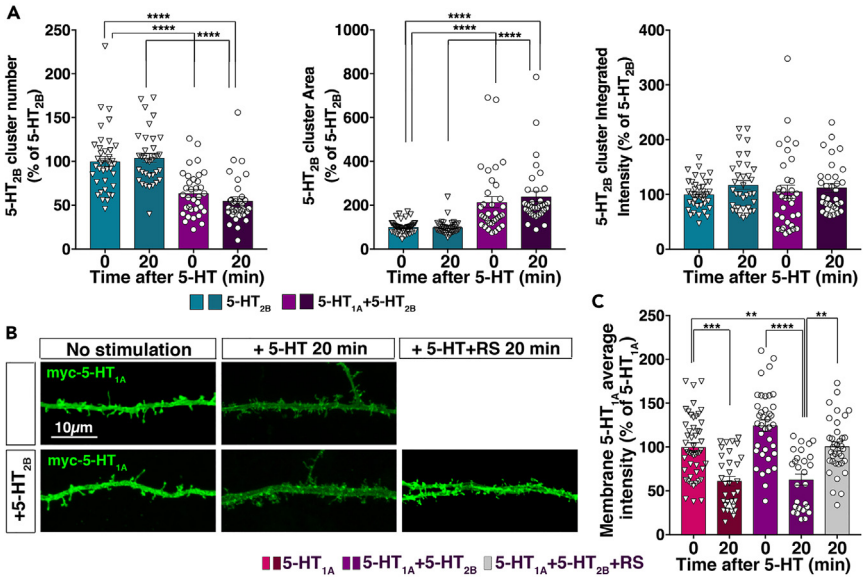

Figure 6. 5-HT stimulation of 5-HT$_{1A}$ and 5-HT$_{2B}$ expressed separately or in combination differentially affects their membrane expression and clustering

(A) Quantification of 5-HT$_{2B}$ membrane clustering following 5-HT stimulation in the presence or not of 5-HT$_{1A}$. In the presence of 5-HT$_{1A}$, the number of 5-HT$_{2B}$ clusters decreased as revealed by Kruskal-Wallis test, $p < 0.0001$, followed by Dunn's multiple comparisons test; $p < 0.0001$, t0 5-HT$_{2B}$ vs. t0 5-HT$_{1A}$+5-HT$_{2B}$ and $p < 0.0001$, t0 5-HT$_{2B}$ vs. t20 5-HT$_{1A}$+5-HT$_{2B}$, but 5-HT$_{2B}$ clustering was unaffected upon 5-HT (1 µM) stimulation. In the presence of 5-HT$_{1A}$, 5-HT$_{2B}$ cluster area increased, as revealed by Kruskal-Wallis test, $p < 0.0001$, followed by Dunn's multiple comparisons test, $p < 0.0001$, t0 5-HT$_{2B}$ vs. t0 5-HT$_{1A}$+5-HT$_{2B}$ and $p < 0.0001$, t0 5-HT$_{2B}$ vs. t20 5-HT$_{1A}$+5-HT$_{2B}$, but was unaffected upon 5-HT stimulation; their molecular density (integrated intensity) was not modified by 5-HT stimulation from 0 to 20 min in the absence or presence of 5-HT$_{1A}$. Data are expressed as percentage of their respective values at t0. (n = 30–39 dendrites from 4 independent cell cultures).

(B) Images of 5-HT$_{1A}$ membrane expression acquired by confocal microscopy. Top, 5-HT$_{1A}$ (green) expression at the dendritic membrane in the absence of 5-HT$_{2B}$ and before or 20 min after 5-HT stimulation. Bottom, 5-HT$_{1A}$ expression at the dendritic membrane in the presence of 5-HT$_{2B}$ and before, 20 min after 5-HT stimulation (1 µM) or 20 min after 5-HT stimulation in the presence of the 5-HT$_{2B}$ antagonist RS (1 µM). Scale bar, 10 µm.

(C) Quantification of 5-HT$_{1A}$ membrane expression after 5-HT stimulation in the absence or presence of 5-HT$_{2B}$. The intensity of 5-HT$_{1A}$ at the neuronal membrane was decreased by 5-HT stimulation as revealed by Kruskal-Wallis test, $p < 0.0001$, followed by Dunn's multiple comparisons test, $p = 0.0003$, t0 5-HT$_{1A}$ vs. t20 5-HT$_{1A}$. Similarly, in the presence of 5-HT$_{2B}$, the 5-HT$_{1A}$ membrane expression was decreased upon 5-HT stimulation, $p < 0.0001$, t0 5-HT$_{1A}$+5-HT$_{2B}$ vs. t20 5-HT$_{1A}$+5-HT$_{2B}$, but remained unaffected upon 5-HT stimulation in the presence of 5-HT$_{2B}$ antagonist RS. n = 27–50 dendrites from 4 independent cell cultures. Data are expressed as percentage of their respective values at t0.

****$p < 0.0001$, ***$p < 0.001$, **$p < 0.01$, *$p < 0.05$. Individual values are presented with mean ± SEM.

Flag-tagged-5-HT$_{1A}$ and HA-tagged-5-HT$_{2B}$ together (Figure S2) in DR 5-HT neurons as schematized on (Figure 7A) (See STAR methods). Confocal images of DR brainstem sections from these mice at low and intermediate magnification showed a fairly good colocalization of both receptors around cell bodies and proximal dendrites (Figure 7B). Quantification analysis of confocal images of DR sections from these mice at high magnification revealed colocalization of both receptors in the somatodendritic compartment of 5-HT neurons (degree of overlap for 5-HT$_{2B}$ over 5-HT$_{1A}$ of 0.462 ± 0.053 and for 5-HT$_{1A}$ over 5-HT$_{2B}$ of 0.465 ± 0.087) (Figure 7C) (See STAR methods).

The serotonergic tone of the DR neurons is known to be negatively regulated by 5-HT$_{1A}$ and activation of 5-HT$_{2B}$ by BW can increase 5-HT neurons firing activity.[24] To investigate putative contribution of these receptor interactions on the firing of 5-HT neurons, we performed patch-clamp recording on identified 5-HT neurons of acute brainstem slices from either control mice or mice selectively lacking 5-HT$_{2B}$ expression in 5-HT neurons. For this purpose, we used as control GFP^{5-HT} mice and 2B-KO^{5-HT}::GFP^{5-HT} mice, both of which expressing GFP exclusively by 5-HT neurons, and studied action potential frequency in response to depolarizing current steps (See STAR methods). Basal Frequency-Intensity (F-I) curves did not differ

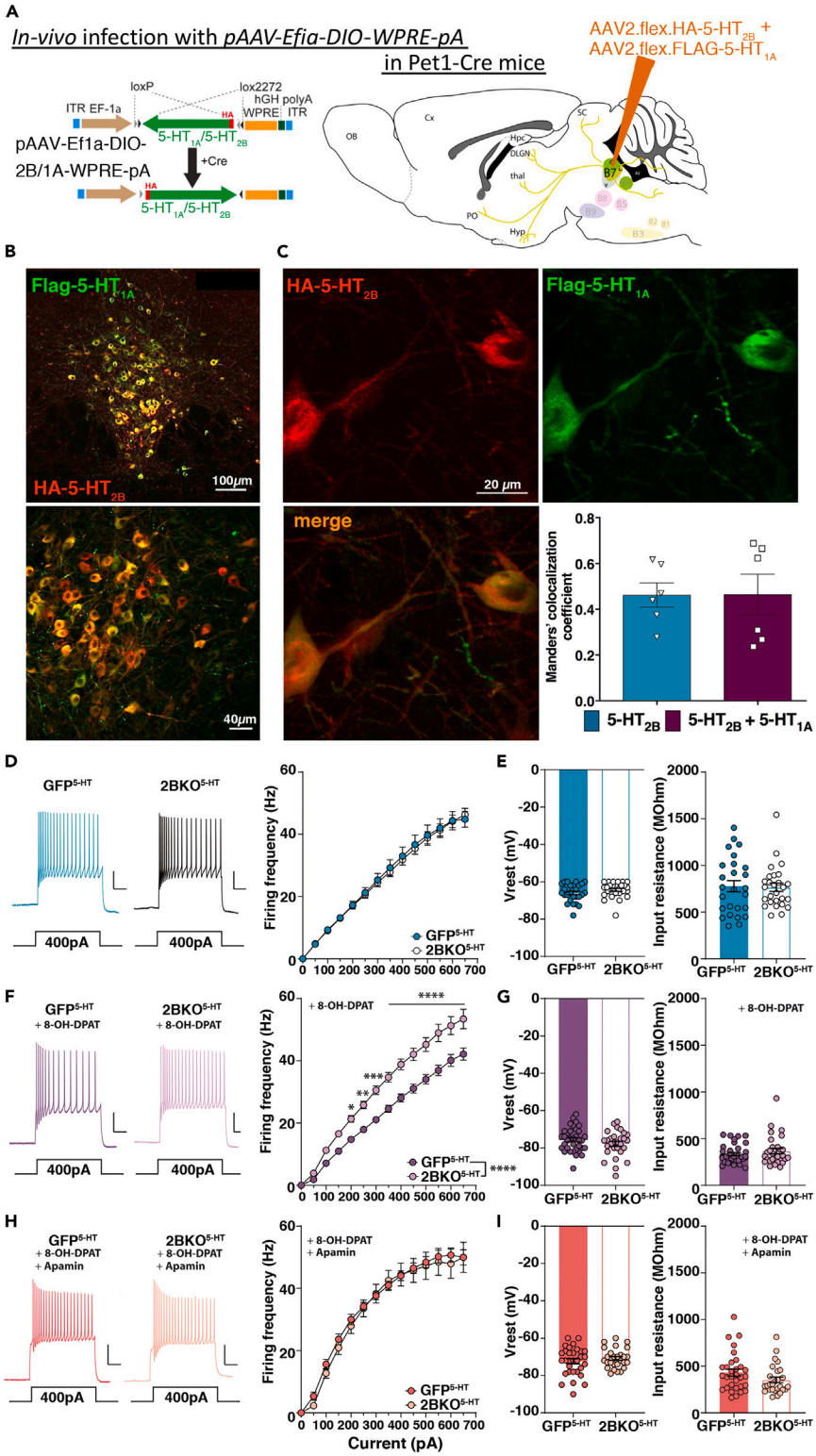

Figure 7. Colocalization of 5-HT$_{1A}$ and 5-HT$_{2B}$ in somatodendritic compartment of 5-HT neurons and co-regulation of their firing activity through SK channels

(A) Schematic of AAVs injection in B7 raphe nucleus from Pet1-GFP mice, to overexpress HA-5-HT$_{2B}$ and FLAG-5-HT$_{1A}$ into 5-HT neuron. Left: map of DIO-AAV construct that allows Cre-mediated expression of the tagged receptor. Right

Figure 7. *Continued*

AAV-DIO-HA5-HT_{2B} and AAV-DIO-FLAG5-HT_{1A} were unilaterally co-injected into B7 raphe nucleus of Pet1-GFP mice to expressed both receptors specifically in dorsal raphe 5-HT neurons.

(B) Mouse brainstem sections were examined to assess the distribution of FLAG-tagged 5-HT_{1A} and HA-tagged 5-HT_{2B} expressed specifically in 5-HT neurons. Images of dorsal raphe 5-HT neurons labeled with anti-Flag (green) and anti-HA (red) antibodies, at increasing magnifications (Top and lower panels).

(C) Analysis of confocal images taken at higher magnification. Similar colocalization of both receptors was observed in the somatodendritic compartment (Upper right panel). (n = 6 images, about 18 cells from 3 independent infections). Scale bars, 100, 40, and 20 μm, as indicated.

(D) Left, sample spike trains evoked by a 400pA current injection in slices from GFP^{5-HT} and 2B-KO^{5-HT}::GFP^{5-HT} mice; scale: 25pA/100 ms. Right, F-I curve (mean ± SEM) for GFP^{5-HT} (n = 26 neurons, 1–2 neurons per slice, 3-4 slice from 7 mice) and 2B-KO^{5-HT}::GFP^{5-HT} 5-HT neurons (n = 27 neurons, 1–2 neurons per slice, 3-4 slice from 6 mice); two-way RM ANOVA, genotype effect, not significant p = 0.8715.

(E) Resting membrane potential (Vrest) and input resistance in GFP^{5-HT} and 2B-KO^{5-HT}::GFP^{5-HT} 5-HT neurons. Bars represent the mean ± SEM; circles show individual recordings.

(F) Left, same as in (D) in presence of 8-OH-DPAT (30 nM), a 5-HT_{1A} selective agonist. Right, F-I curve (mean ± SEM) for GFP^{5-HT} (n = 35 neurons, 1–2 neurons per slice, 3-4 slice from 5 mice) and 2B-KO^{5-HT}::GFP^{5-HT} 5-HT neurons (n = 29 neurons, 1–2 neurons per slice, 3-4 slice from 4 mice) in the presence of 8-OH-DPAT (30 nM); two-way RM ANOVA revealed a significant increase in firing rate of 2B-KO^{5-HT}::GFP^{5-HT}, genotype effect $p < 0.0001$; Sidak's *post hoc* test* p = 0.0274, **p = 0.0028, ***p = 0.0001, ****$p < 0.0001$.

(G) Same as in (E) in the presence of 8-OH-DPAT (30 nM).

(H) Left, same as in (D) and (F) in the presence of 8-OH-DPAT (30 nM) and apamin (20 nM), a selective SK channel blocker. Right, F–I curve (mean ± SEM) for GFP^{5-HT} (n = 31 neurons, 1–2 neurons per slice, 3-4 slice from 4 individual mice) and 2B-KO^{5-HT}::GFP^{5-HT} 5-HT neurons (n = 27 neurons, 1–2 neurons per slice, 3-4 slice from 3 mice) in the presence of 8-OH-DPAT (30 nM) and apamin (20 nM); two-way RM ANOVA, no genotype effect p = 0.6979.

(I) Same as in (D) and (F) in the presence of 8-OH-DPAT (30 nM) and apamin (20 nM).

between GFP^{5-HT} and 2B-KO^{5-HT}::GFP^{5-HT} 5-HT neurons (Figure 7D), nor the resting membrane potential and input resistance (Figure 7E). In the presence of the 5-HT_{1A} agonist 8-OH-DPAT (30 nM), the firing frequency of GFP^{5-HT} 5-HT neurons was decreased; the firing frequency of 2B-KO^{5-HT}::GFP^{5-HT} 5-HT neurons became significantly higher than that of GFP^{5-HT} 5-HT neurons (Figure 7F), or of unstimulated 2B-KO^{5-HT}::GFP^{5-HT} 5-HT neurons (not illustrated); the resting membrane potential and input resistance remained similar (Figure 7G), but different from unstimulated neurons, with a reduction in resting potential (−65 mV vs. −77 mV) and in input resistance (771 MOhm vs. 350 MOhm) (Figure S1). SK channels are responsible for mAHPs, that control the tonic firing of DR 5-HT neurons. When a selective SK2/3 channel blocker, apamin (20 nM) was applied together with 8-OH-DPAT (30 nM), F-I curves for GFP^{5-HT} and 2B-KO^{5-HT}::GFP^{5-HT} 5-HT neurons became again similar (Figure 7H) and higher than the unstimulated condition, with resting membrane potential and input resistance remaining similar and close to the value obtained after 8-OHDPAT stimulation (Figure 7I). These results indicate that, in the absence of 5-HT_{2B} (i.e., in brainstem slices from 2B-KO^{5-HT}::GFP^{5-HT} mice), 5-HT neuron firing activity is increased upon 5-HT_{1A} stimulation by 8-OH-DPAT, when 5-HT_{1A} can be internalized. In the presence of 5-HT_{2B} (i.e., in GFP^{5-HT} mice), 5-HT neuron firing activity is decreased when 8-OH-DPAT cannot trigger internalization of 5-HT_{1A}, supporting a link between receptor functions and trafficking.

DISCUSSION

Combined with our previous investigations about 5-HT_{2B} functions in 5-HT neurons[24] and extensive studies on 5-HT_{1A} activity as autoreceptors of these neurons, the present work demonstrates that 5-HT_{1A}/5-HT_{2B} interactions are implicated in the regulation of serotonergic tone, which is a prime importance for mood disorders. We found that 5-HT_{1A} and 5-HT_{2B} are colocalized upon overexpression in hippocampal cultures and in 5-HT neurons *in vivo*, and can interact together to form dimers. Coexpression of these two receptors impacts on their membrane expression level and/or concentration in clusters, which can be further regulated by stimulation with various agonists.

Different techniques allowed us to validate the reciprocal effects of 5-HT_{1A} and 5-HT_{2B} on their subcellular distribution. Confocal microscopy was used to analyze and compare, in various conditions, the number of clusters, their size and the density of receptors per cluster. With a resolution up to ~20 nm, STORM allows an accurate analysis of receptor spatial distribution and confirmed that 5-HT_{2B} are locally concentrated in clusters at the membrane of hippocampal neurons. Moreover, this technique confirmed that stimulation of 5-HT_{2B} by its selective agonist, BW, triggers its aggregation into larger and denser clusters (summarized in

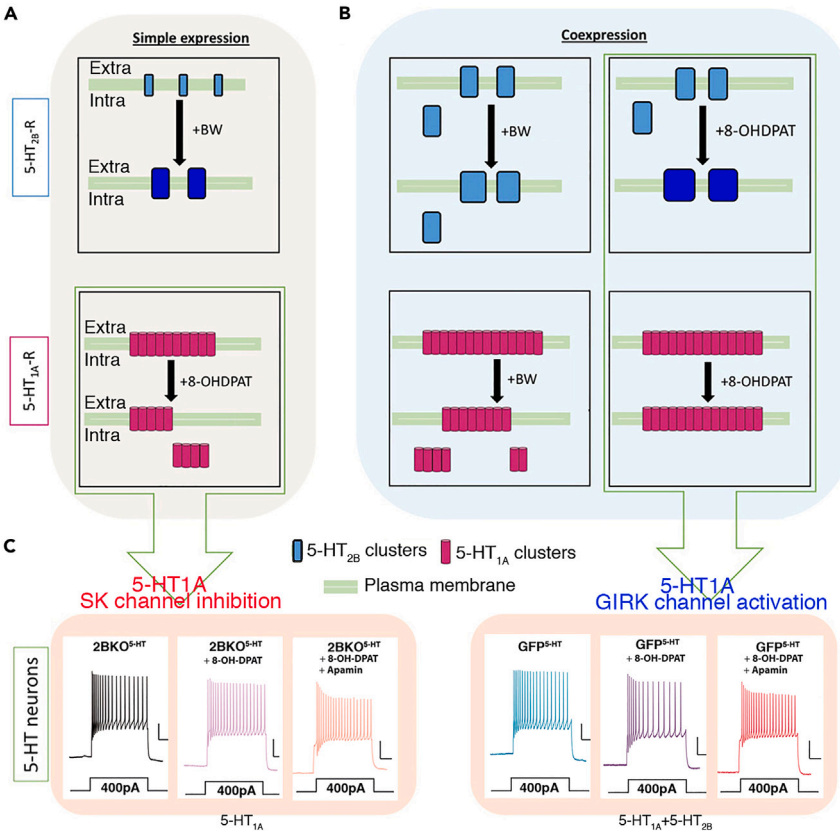

Figure 8. Co-expression of 5-HT$_{1A}$ and 5-HT$_{2B}$ impacts their membrane expression, clustering, and physiological function

(A) Separate expression of 5-HT$_{1A}$ or 5-HT$_{2B}$. Top, BW stimulation increases 5-HT$_{2B}$ clustering. Bottom, 8-OH-DPAT stimulation decreases membrane expression of 5-HT$_{1A}$ probably via endocytosis.

(B) Co-expression of 5-HT$_{2B}$ and 5-HT$_{1A}$ and their stimulation affects the membrane expression of both receptors. Top, 5-HT$_{1A}$ expression increases 5-HT$_{2B}$ clustering. The 5-HT$_{2B}$ stimulation by BW does not reverse the clustering effect of 5-HT$_{1A}$ on 5-HT$_{2B}$. Stimulation by 8-OH-DPAT of 5-HT$_{1A}$ further increases 5-HT$_{2B}$ clustering. Bottom, Coexpression of 5-HT$_{2B}$ increases 5-HT$_{1A}$ membrane expression. No further change in membrane expression of 5-HT$_{1A}$ is detected upon its stimulation with 8-OH-DPAT, but 5-HT$_{2B}$ stimulation by BW decreases 5-HT$_{1A}$ membrane expression.

(C) The 5-HT$_{2B}$/5-HT$_{1A}$ co-expression/interaction regulates the excitability of 5-HT neurons. In the absence of 5-HT$_{2B}$ (Separated expression, i.e., 2B-KO5-HT, left), 5-HT neuron firing activity is increased upon 5-HT$_{1A}$ stimulation by 8-OH-DPAT, independently of SK channels blockade by apamin. By contrast, upon co-expression of 5-HT$_{2B}$ (Co-expression, i.e., WT, right), 5-HT neuron firing activity is decreased by 8-OH-DPAT unless SK channels are blocked by apamin.

Accumulation of 5-HT$_{2B}$ in cluster is in blue with variations in size and intensity. Membrane association of 5-HT$_{1A}$ in small cluster is in red with internalization at intracellular compartments (Intra). Plasma membrane is in green.

Figure 8A). 5-HT$_{1A}$ coexpression also increases 5-HT$_{2B}$ clustering, as assessed by the significant decrease in the number but increase in the area of 5-HT$_{2B}$ clusters, and 5-HT$_{2B}$ aggregation is further enhanced upon selective stimulation of either 5-HT$_{2B}$ (by BW as evidenced by STORM) or 5-HT$_{1A}$ (by 8-OH-DPAT) (Figure 8B). On the other hand, stimulation of 5-HT$_{1A}$ by its selective agonist 8-OH-DPAT decreases its membrane expression if they are expressed alone (Figure 8A), but this down-regulating effect of 8-OH-DPAT on 5-HT$_{1A}$ is not observed when 5-HT$_{2B}$ is coexpressed (Figure 8B). It has been shown that 5-HT$_{1A}$ autoreceptors desensitize and are internalized upon stimulation[34] and especially after chronic exposure to high extracellular concentration of 5-HT, a condition induced for example by chronic SSRI treatment.[18]

The mechanisms of 5-HT$_{1A}$ internalization involve phosphorylation by PKA and PKC since phosphorylation sites were identified in 5-HT$_{1A}$.[35] Stimulation by 8-OH-DPAT of 5-HT$_{1A}$ recruits β-arrestin2,[5] which, with GRK2, triggers its internalization via clathrin-coated pits,[36] and signaling to ERK1/2.[37] Concerning 5-HT$_{2B}$, we showed that 5-HT$_{2B}$ internalization was dependent on β-arrestin-2, GRK2,3 and clathrin when

stimulated either by 5-HT or BW, although stimulation by BW internalized 5-HT_{2B} more than twice faster than 5-HT.[38] Here, we show that internalization of 5-HT_{1A} by 8-OH-DPAT is prevented by the presence of 5-HT_{2B}. 5-HT_{1A} internalization is observed only when 5-HT_{2B} is stimulated by BW or by 5-HT and 5-HT_{2B} internalization is insensitive to the presence of 5-HT_{1A}. This finding supports a competition between 5-HT_{1A} and 5-HT_{2B} for desensitization machinery: 5-HT_{1A} internalization being prevented unless 5-HT_{2B} are stimulated. Of note, PKC, which can be activated by 5-HT_{2B}, was shown to induce a rapid phosphorylation of 5-HT_{1A}.[35] Nevertheless, the precise mechanisms underlying internalization and desensitization of 5-HT_{1A} and 5-HT_{2B} in 5-HT neurons remain to be identified.

Oligomerization of GPCRs is a well-documented process that can be essential for their trafficking to the plasma membrane, agonist binding, and signaling.[39,40] Metabotropic 5-HT are able to form homo or heterodimers with each other or with non-5-HT receptors,[26] which can impact on their function. For example, 5-HT_{1A}/5-HT_7 heterodimerization decreases Gαi and subsequent GIRK activation downstream of 5-HT_{1A} stimulation, without affecting 5-HT_7 signaling pathway.[32] 5-HT_{1A} and 5-HT_{2A} (close relative to 5-HT_{2B}) can form oligomers[41] in pyramidal neurons of the prefrontal cortex. Coexpression of these two receptors triggers 5-HT_{1A}-dependent inhibitory responses, 5-HT_{2A}-dependent excitatory responses, and biphasic responses in which excitation follows a brief inhibition likely depending on respective expression levels of these receptors.[42,43] In cells coexpressing 5-HT_{1B} (close relative to 5-HT_{1A}) and 5-HT_{2B}, and in the absence of direct interaction, stimulation by 5-HT makes 5-HT_{2B} to internalize via its classic clathrin pathways but also via 5-HT_{1B}-triggered GRK2,3 activation and Caveolin1-dependent pathways.[38] Here, we show that coexpression of 5-HT_{1A} and 5-HT_{2B}, despite no apparent impact on their classical second messenger signaling, has an effect on the expression level of both receptors at the plasma membrane (Figure 8B). The specific interacting sequence in the heteromer between the 5-HT_{2B} and the 5-HT_{1A} remains to be identified.

Coexpression of 5-HT_{1A} with 5-HT_{2B} favors the clustering of 5-HT_{2B}, mimicking the effect of 5-HT_{2B} stimulation, and this is further enhanced by selective stimulation of 5-HT_{1A} with 8-OH-DPAT. We can thus conclude that 5-HT_{1A}, without or with stimulation, can control 5-HT_{2B} membrane clustering. Reciprocally, while homologous 5-HT_{1A} agonist stimulation by 8-OH-DPAT decreases 5-HT_{1A} membrane expression if this receptor is expressed alone, the coexpression with 5-HT_{2B} increases 5-HT_{1A} membrane level and maintains it at the neuronal membrane, counteracting the effect of 5-HT_{1A} stimulation by its own agonist 8-OH-DPAT (Figure 8B). Therefore, the dynamic regulation of 5-HT_{1A} membrane expression not only depends on the ligand but also on the panel of receptors expressed by the neuron. In addition, we show that 5-HT, the physiological ligand of 5-HT_{1A} and 5-HT_{2B}, has no significant impact on the distribution of 5-HT_{2B} coexpressed with 5-HT_{1A}. Interestingly, we found that 5-HT stimulation abolishes 5-HT_{2B} positive effect on 5-HT_{1A} membrane expression, and decreases 5-HT_{1A} membrane expression level. This decrease in 5-HT_{1A} membrane expression is entirely 5-HT_{2B}-dependent since it can be restored by applying the highly selective 5-HT_{2B} antagonist RS, confirming the observation that BW reduces 5-HT_{1A} membrane expression only in the presence of 5-HT_{2B}. Together, our results demonstrate that modulation of 5-HT_{1A} membrane expression can be triggered not only by its own stimulation, but also through 5-HT_{2B} activation, confirming their functional crosstalk.

We previously reported that *in vivo* injection of BW attenuated 8-OH-DPAT-induced hypothermia and inhibition of 5-HT neurons firing. These two effects of 8-OH-DPAT are attributed to the activation of 5-HT_{1A} expressed by 5-HT neurons. These data suggested that 5-HT_{2B} counteracted 5-HT_{1A} negative effects on 5-HT neurons.[24] These 5-HT_{2B} positive effects were also substantiated by cell-attached electrophysiological recording showing that 5-HT_{2B} activation by BW increased 5-HT neurons firing activity.[24] Here, using current-clamp recording in *ex vivo* identified 5-HT neurons, we observed that the increase in firing frequency of action potentials upon raising current steps was similar in GFP^{5-HT} mice and in 2B-KO^{5-HT}::GFP^{5-HT} mice. Stimulation by 8-OH-DPAT decreased the firing frequency of 5-HT neurons from GFP^{5-HT} mice, i.e., in the presence of 5-HT_{2B} and 5-HT_{1A}. The coexpression of 5-HT_{1A} with 5-HT_{2B} increases 5-HT_{1A} membrane expression, and blocks its internalization upon 8-OH-DPAT stimulation (Figure 8C), supporting that 5-HT_{2B} is important to stabilize 5-HT_{1A} at the plasma membrane, and to limit its agonist-induced internalization. This coexpression likely favors 5-HT_{1A}-dependent activation of GIRK channels. The basal GIRK conductance contributes the intrinsic membrane properties of DR neurons and, in particular, the GIRK2 subunit contributes to set the resting membrane potential and input resistance of DR neurons.[44] It is therefore, not surprising to find that 8-OHDPAT triggered a reduction in resting potential and in

input resistance (Figure S1), which were not further affected by apamin since stimulation of 5-HT$_{1A}$ is known to activate GIRK channels.[11] By contrast, stimulation by 8-OH-DPAT in the presence of apamin significantly increased the firing frequency of 5-HT neurons from GFP^{5-HT} mice compared to unstimulated neurons, and similar to that of 2B-KO^{5-HT}::GFP^{5-HT} neurons i.e., in the absence of 5-HT$_{2B}$. This finding supports that in the absence of 5-HT$_{2B}$, 8-OH-DPAT triggers internalization of 5-HT$_{1A}$ and favors its coupling to SK inhibition (Figure 8C) as previously reported[16]; in the presence of 5-HT$_{2B}$, 8-OH-DPAT reduces the ability of 5-HT$_{1A}$ to couple to SK channel inhibition. The observation that coexpression with 5-HT$_{1A}$ increases the size of 5-HT$_{2B}$ clusters that is potentiated by 8-OH-DPAT, may finally support the 5-HT$_{2B}$ ability to couple to SK channel inhibition in this condition, likely by competition with 5-HT$_{1A}$.

Using current-clamp recordings, we previously showed that overexpression of 5-HT$_{2B}$ in 5-HT neuron triggered a significant increase in the basal (non-stimulated) firing frequency compared to controls.[24] Apamin was shown to increase the burst firing of DR 5-HT neurons leading to increased 5-HT release[14] in a similar way as the SSRI fluoxetine[45] or as the 5-HT$_{2B}$ agonist BW.[21,24] Furthermore, mice exposed to chronic social isolation develop depressive-like state that can be reversed by SSRIs only in the presence of 5-HT$_{2B}$,[46] or by apamin, which regulates 5-HT firing pattern.[47] Together, these data support that interaction between 5-HT$_{2B}$/5-HT$_{1A}$ and their stoichiometry are required to control proper firing of 5-HT neurons by regulating mAHP that condition SSRIs efficacy.

Limitations of the study

In this work, intracellular interactions between 5-HT$_{1A}$ and 5-HT$_{2B}$ data are mainly based on overexpression studies either on transfected cells and hippocampal neurons or on *in vivo* infected 5-HT neurons. When reliable antibodies will be available, it will be necessary to further validate these findings on endogenous receptors *in vivo*. Although established on *ex vivo* endogenously expressed receptors, it remains to be determined *in vivo* if 5-HT$_{2B}$ stimulation controls directly (e.g., by PKC activation and thus by phosphorylation) SK channels, and/or 5-HT$_{1A}$ or if this regulation is relying exclusively on 5-HT$_{1A}$/5-HT$_{2B}$ dimeric interactions and/or competition to common effectors.

STAR★METHODS

Detailed methods are provided in the online version of this paper and include the following:

- KEY RESOURCES TABLE
- RESOURCE AVAILABILITY
  - Lead contact
  - Materials availability
  - Data and code availability
- EXPERIMENTAL MODEL AND SUBJECT DETAILS
  - Animals
  - Ethical statement
- METHODS DETAILS
  - Viral constructs and stereotaxic injection
  - Culture of COS-7 cells
  - Co-immunoprecipitation
  - Bioluminescence resonance energy transfer (BRET)
  - Binding experiments
  - Second messenger measurements
  - HTRF IP accumulation
  - Surface biotinylation
  - Western blotting
  - Hippocampal neuronal culture and transfection
  - Immunostaining
  - Fluorescence image acquisition and cluster analyses
  - Quantitative colocalization analysis
  - STORM imaging
  - Electrophysiology
- QUANTIFICATION AND STATISTICAL ANALYSIS
  - Experimental design and statistical analysis

SUPPLEMENTAL INFORMATION

Supplemental information can be found online at https://doi.org/10.1016/j.isci.2023.107401.

ACKNOWLEDGMENTS

We thank the *Cell* and *Tissue Imaging Facility* of the Institut du Fer à Moulin (namely Theano Eirinopoulou, Mythili Savariradjane), where all image acquisitions and analyses have been performed, Aude Muzerelle for help with stereotaxic viral injections, and the staff of the IFM animal facility (namely Baptiste Lecomte, Gaël Grannec, François Baudoin, Anna-Sophia Lourenço, Emma Courteau and Eloise Marsan). This work has been supported by grants from the Agence Nationale de la Recherche (ANR-17-CE16-0008, ANR-11-IDEX-0004-02), the Fondation pour la Recherche Médicale (Equipe FRM DEQ2014039529 to L.M and R22184DD to S.L.) and the Fédération pour la Recherche sur le Cerveau (FRC-2019-19F10 to L.M and R20020DD to S.L.).

AUTHOR CONTRIBUTIONS

L.M., S.L., C.L., and A.R. designed the studies. L.M., A.B., C.L., and A.R wrote the manuscript, and all authors revised it. A.B., I.M., X.M., and M.R. performed pharmacological studies, BRET experiments, stereotaxy and animal experiments, immunofluorescence, image acquisition and analysis with the help of S.L., C.D., and C.L. performed and analyzed electrophysiological experiments. A.B., S.L., L.M., and A.R. performed data analysis.

DECLARATION OF INTERESTS

The authors declare no conflict of interest.

Received: April 3, 2023
Revised: May 26, 2023
Accepted: July 12, 2023
Published: July 15, 2023

REFERENCES

1. Arango, V., Huang, Y.-Y., Underwood, M.D., and Mann, J.J. (2003). Genetics of the serotonergic system in suicidal behavior. J. Psychol. Res. *37*, 375–386. https://doi.org/10.1016/s0022-3956(03)00048-7.

2. Mann, J.J. (1999). Role of the serotonergic system in the pathogenesis of major depression and suicidal behavior. Neuropsychopharmacology *21*, 99S–105S. https://doi.org/10.1016/S0893-133X(99)00040-8.

3. Marazziti, D. (2017). Understanding the role of serotonin in psychiatric diseases. F1000Res. *6*, 180. https://doi.org/10.12688/f1000research.10094.1.

4. Lin, S.L., Setya, S., Johnson-Farley, N.N., and Cowen, D.S. (2002). Differential coupling of 5-HT(1) receptors to G proteins of the G(i) family. Br. J. Pharmacol. *136*, 1072–1078. https://doi.org/10.1038/sj.bjp.0704809.

5. Albert, P.R., and Vahid-Ansari, F. (2019). The 5-HT1A receptor: signaling to behavior. Biochimie *161*, 34–45. https://doi.org/10.1016/j.biochi.2018.10.015.

6. Andrade, R., Huereca, D., Lyons, J.G., Andrade, E.M., and Mcgregor, K.M. (2015). 5-HT1A receptor-mediated autoinhibition and the control of serotonergic cell firing. ACS Chem. Neurosci. *6*, 1110–1115. https://doi.org/10.1021/acschemneuro.5b00034.

7. Garcia-Garcia, A.L., Newman-Tancredi, A., and Leonardo, E.D. (2014). 5-HT1A receptors in mood and anxiety: recent insights into autoreceptor versus heteroreceptor function. Psychopharmacology *231*, 623–636. https://doi.org/10.1007/s00213-013-3389-x.

8. McDevitt, R.A., and Neumaier, J.F. (2011). Regulation of dorsal raphe nucleus function by serotonin autoreceptors: a behavioral perspective. J. Chem. Neuroanat. *41*, 234–246. https://doi.org/10.1016/j.jchemneu.2011.05.001.

9. Courtney, N.A., and Ford, C.P. (2016). Mechanisms of 5-HT1A receptor-mediated transmission in dorsal raphe serotonin neurons. J. Physiol. *594*, 953–965. https://doi.org/10.1113/JP271716.

10. Llamosas, N., Bruzos-Cidón, C., Rodríguez, J.J., Ugedo, L., and Torrecilla, M. (2015). Deletion of GIRK2 subunit of GIRK channels alters the 5-HT1A receptor-mediated signaling and results in a depression-resistant behavior. Int. J. Neuropsychopharmacol. *18*, pyv051. https://doi.org/10.1093/ijnp/pyv051.

11. Montalbano, A., Corradetti, R., and Mlinar, B. (2015). Pharmacological characterization of 5-HT1A autoreceptor-coupled GIRK channels in rat dorsal raphe 5-HT neurons. PLoS One *10*, e0140369. https://doi.org/10.1371/journal.pone.0140369.

12. Heusler, P., Pauwels, P.J., Wurch, T., Newman-Tancredi, A., Tytgat, J., Colpaert, F.C., and Cussac, D. (2005). Differential ion current activation by human 5-HT(1A) receptors in Xenopus oocytes: evidence for agonist-directed trafficking of receptor signalling. Neuropharmacology *49*, 963–976. https://doi.org/10.1016/j.neuropharm.2005.05.001.

13. Kirby, L.G., Pernar, L., Valentino, R.J., and Beck, S.G. (2003). Distinguishing characteristics of serotonin and non-serotonin-containing cells in the dorsal raphe nucleus: electrophysiological and immunohistochemical studies. Neuroscience *116*, 669–683.

14. Crespi, F. (2009). Apamin increases 5-HT cell firing in raphe dorsalis and extracellular 5-HT levels in amygdala: a concomitant in vivo study in anesthetized rats. Brain Res. *1281*, 35–46. https://doi.org/10.1016/j.brainres.2009.05.021.

15. Rouchet, N., Waroux, O., Lamy, C., Massotte, L., Scuvée-Moreau, J., Liégeois, J.F., and Seutin, V. (2008). SK channel blockade promotes burst firing in dorsal raphe serotonergic neurons. Eur. J. Neurosci. *28*, 1108–1115. https://doi.org/10.1111/j.1460-9568.2008.06430.x.

16. Grunnet, M., Jespersen, T., and Perrier, J.-F. (2004). 5-HT1A receptors modulate small-conductance Ca2+-activated K+ channels.

J. Neurosci. Res. *78*, 845–854. https://doi.org/10.1002/jnr.20318.

17. Riad, M., Watkins, K.C., Doucet, E., Hamon, M., and Descarries, L. (2001). Agonist-induced internalization of serotonin-1a receptors in the dorsal raphe nucleus (autoreceptors) but not hippocampus (heteroreceptors). J. Neurosci. *21*, 8378–8386.

18. Soiza-Reilly, M., Goodfellow, N.M., Lambe, E.K., and Commons, K.G. (2015). Enhanced 5-HT1A receptor-dependent feedback control over dorsal raphe serotonin neurons in the SERT knockout mouse. Neuropharmacology *89*, 185–192. https://doi.org/10.1016/j.neuropharm.2014.09.017.

19. Bevilacqua, L., Doly, S., Kaprio, J., Yuan, Q., Tikkanen, R., Paunio, T., Zhou, Z., Wedenoja, J., Maroteaux, L., Diaz, S., et al. (2010). A population-specific HTR2B stop codon predisposes to severe impulsivity. Nature *468*, 1061–1066.

20. Tikkanen, R., Tiihonen, J., Rautiainen, M.R., Paunio, T., Bevilacqua, L., Panarsky, R., Goldman, D., and Virkkunen, M. (2015). Impulsive alcohol-related risk-behavior and emotional dysregulation among individuals with a serotonin 2B receptor stop codon. Transl. Psychiatry *5*, e681. https://doi.org/10.1038/tp.2015.170.

21. Diaz, S.L., Doly, S., Narboux-Nême, N., Fernández, S., Mazot, P., Banas, S.M., Boutourlinsky, K., Moutkine, I., Belmer, A., Roumier, A., and Maroteaux, L. (2012). 5-HT2B receptors are required for serotonin-selective antidepressant actions. Mol. Psychiatry *17*, 154–163.

22. Niederkofler, V., Asher, T.E., Okaty, B.W., Rood, B.D., Narayan, A., Hwa, L.S., Beck, S.G., Miczek, K.A., and Dymecki, S.M. (2016). Identification of serotonergic neuronal modules that affect aggressive behavior. Cell Rep. *17*, 1934–1949. https://doi.org/10.1016/j.celrep.2016.10.063.

23. Okaty, B.W., Sturrock, N., Escobedo Lozoya, Y., Chang, Y., Senft, R.A., Lyon, K.A., Alekseyenko, O.V., and Dymecki, S.M. (2020). A single-cell transcriptomic and anatomic atlas of mouse dorsal raphe Pet1 neurons. Elife *9*, e55523. https://doi.org/10.7554/eLife.55523.

24. Belmer, A., Quentin, E., Diaz, S.L., Guiard, B.P., Fernandez, S.P., Doly, S., Banas, S.M., Pitychoutis, P.M., Moutkine, I., Muzerelle, A., et al. (2018). Positive regulation of raphe serotonin neurons by serotonin 2B receptors. Neuropsychopharmacology *43*, 1623–1632. https://doi.org/10.1038/s41386-018-0013-0.

25. Kidd, E.J., Garratt, J.C., and Marsden, C.A. (1991). Effects of repeated treatment with 1-(2,5-dimethoxy-4-iodophenyl)-2-aminopropane (DOI) on the autoregulatory control of dorsal raphe 5-HT neuronal firing and cortical 5-HT release. Eur. J. Pharmacol. *200*, 131–139.

26. Maroteaux, L., Béchade, C., and Roumier, A. (2019). Dimers of serotonin receptors: impact on ligand affinity and signaling. Biochimie *161*, 22–33. https://doi.org/10.1016/j.biochi.2019.01.009.

27. Moutkine, I., Quentin, E., Guiard, B.P., Maroteaux, L., and Doly, S. (2017). Heterodimers of serotonin receptor subtypes 2 are driven by 5-HT2C protomers. J. Biol. Chem. *292*, 6352–6368. https://doi.org/10.1074/jbc.M117.779041.

28. Fagni, L., Worley, P.F., and Ango, F. (2002). Homer as both a scaffold and transduction molecule. Sci. STKE *2002*, re8. https://doi.org/10.1126/stke.2002.137.re8.

29. Benhadda, A., Quentin, E., Moutkine, I., Chanrion, B., Russeau, M., Marin, P., Levi, S., and Maroteaux, L. (2021). Serotonin 2B receptor by interacting with NMDA receptor and CIPP protein complex may control structural plasticity at glutamatergic synapses. ACS Chem. Neurosci. *12*, 1133–1149. https://doi.org/10.1021/acschemneuro.0c00638.

30. Kia, H.K., Miquel, M.C., Brisorgueil, M.J., Daval, G., Riad, M., el Mestikawy, S., Hamon, M., and Vergé, D. (1996). Immunocytochemical localization of serotonin1A receptors in the rat central nervous system. J. Comp. Neurol. *365*, 289–305. https://doi.org/10.1002/(SICI)1096-9861.

31. Riad, M., Garcia, S., Watkins, K.C., Jodoin, N., Doucet, E., Langlois, X., el Mestikawy, S., Hamon, M., and Descarries, L. (2000). Somatodendritic localization of 5-HT1A and preterminal axonal localization of 5-HT1B serotonin receptors in adult rat brain. J. Comp. Neurol. *417*, 181–194.

32. Renner, U., Zeug, A., Woehler, A., Niebert, M., Dityatev, A., Dityateva, G., Gorinski, N., Guseva, D., Abdel-Galil, D., Fröhlich, M., et al. (2012). Heterodimerization of serotonin receptors 5-HT1A and 5-HT7 differentially regulates receptor signalling and trafficking. J. Cell Sci. *125*, 2486–2499. https://doi.org/10.1242/jcs.101337.

33. Calebiro, D., Koszegi, Z., Lanoiselée, Y., Miljus, T., and O'Brien, S. (2021). G protein-coupled receptor-G protein interactions: a single-molecule perspective. Physiol. Rev. *101*, 857–906. https://doi.org/10.1152/physrev.00021.2020.

34. Bouaziz, E., Emerit, M.B., Vodjdani, G., Gautheron, V., Hamon, M., Darmon, M., and Masson, J. (2014). Neuronal phenotype dependency of agonist-induced internalization of the 5-HT1A serotonin receptor. J. Neurosci. *34*, 282–294. https://doi.org/10.1523/JNEUROSCI.0186-13.2014.

35. Raymond, J.R., Mukhin, Y.V., Gettys, T.W., and Garnovskaya, M.N. (1999). The recombinant 5-HT1A receptor: G protein coupling and signalling pathways. Br. J. Pharmacol. *127*, 1751–1764. https://doi.org/10.1038/sj.bjp.0702723.

36. Heusler, P., Newman-Tancredi, A., Loock, T., and Cussac, D. (2008). Antipsychotics differ in their ability to internalise human dopamine D2S and human serotonin 5-HT1A receptors in HEK293 cells. Eur. J. Pharmacol. *581*, 37–46. https://doi.org/10.1016/j.ejphar.2007.11.046.

37. Della Rocca, G.J., Maudsley, S., Daaka, Y., Lefkowitz, R.J., and Luttrell, L.M. (1999). Pleiotropic coupling of G protein-coupled receptors to the mitogen- activated protein kinase cascade. Role Of focal adhesions and receptor tyrosine kinases. J. Biol. Chem. *274*, 13978–13984.

38. Janoshazi, A., Deraet, M., Callebert, J., Setola, V., Guenther, S., Saubamea, B., Manivet, P., Launay, J.M., and Maroteaux, L. (2007). Modified receptor internalization upon co-expression of 5-HT1B receptor and 5-HT2B receptors. Mol. Pharmacol. *71*, 1463–1474.

39. Herrick-Davis, K. (2013). Functional significance of serotonin receptor dimerization. Exp. Brain Res. *230*, 375–386. https://doi.org/10.1007/s00221-013-3622-1.

40. Faron-Górecka, A., Szlachta, M., Kolasa, M., Solich, J., Górecki, A., Kuśmider, M., Żurawek, D., and Dziedzicka-Wasylewska, M. (2019). Understanding GPCR dimerization. In Receptor-Receptor Interactions, pp. 155–178. https://doi.org/10.1016/bs.mcb.2018.08.005.

41. Borroto-Escuela, D.O., Li, X., Tarakanov, A.O., Savelli, D., Narváez, M., Shumilov, K., Andrade-Talavera, Y., Jimenez-Beristain, A., Pomierny, B., Díaz-Cabiale, Z., et al. (2017). Existence of brain 5-HT1A-5-HT2A isoreceptor complexes with antagonistic allosteric receptor-receptor interactions regulating 5-HT1A receptor recognition. ACS Omega *2*, 4779–4789. https://doi.org/10.1021/acsomega.7b00629.

42. Avesar, D., and Gulledge, A.T. (2012). Selective serotonergic excitation of callosal projection neurons. Front. Neural Circuits *6*, 12. https://doi.org/10.3389/fncir.2012.00012.

43. Ju, A., Fernandez-Arroyo, B., Wu, Y., Jacky, D., and Beyeler, A. (2020). Expression of serotonin 1A and 2A receptors in molecular- and projection-defined neurons of the mouse insular cortex. Mol. Brain *13*, 99. https://doi.org/10.1186/s13041-020-00605-5.

44. Llamosas, N., Ugedo, L., and Torrecilla, M. (2017). Inactivation of GIRK channels weakens the pre- and postsynaptic inhibitory activity in dorsal raphe neurons. Physiol. Rep. *5*, e13141. https://doi.org/10.14814/phy2.13141.

45. Crespi, F. (2010). SK channel blocker apamin attenuates the effect of SSRI fluoxetine upon cell firing in dorsal raphe nucleus: a concomitant electrophysiological and electrochemical in vivo study reveals implications for modulating extracellular 5-HT. Brain Res. *1334*, 1–11. https://doi.org/10.1016/j.brainres.2010.03.081.

46. Diaz, S.L., Narboux-Nême, N., Boutourlinsky, K., Doly, S., and Maroteaux, L. (2016). Mice lacking the serotonin 5-HT2B receptor as an animal model of resistance to selective serotonin reuptake inhibitors antidepressants. Eur. Neuropsychopharmacol. *26*, 265–279. https://doi.org/10.1016/j.euroneuro.2015.12.012.

47. Sargin, D., Oliver, D.K., and Lambe, E.K. (2016). Chronic social isolation reduces 5-HT neuronal activity via upregulated SK3 calcium-activated potassium channels. Elife *5*, e21416. https://doi.org/10.7554/eLife.21416.

48. Scott, M.M., Wylie, C.J., Lerch, J.K., Murphy, R., Lobur, K., Herlitze, S., Jiang, W., Conlon, R.A., Strowbridge, B.W., and Deneris, E.S. (2005). A genetic approach to access serotonin neurons for in vivo and in vitro studies. Proc. Natl. Acad. Sci. USA *102*, 16472–16477. https://doi.org/10.1073/pnas.0504510102.

49. Percie du Sert, N., Hurst, V., Ahluwalia, A., Alam, S., Avey, M.T., Baker, M., Browne, W.J., Clark, A., Cuthill, I.C., Dirnagl, U., et al. (2020). The ARRIVE guidelines 2.0: Updated guidelines for reporting animal research. PLoS Biol. *18*, e3000410. https://doi.org/10.1371/journal.pbio.3000410.

50. Muzerelle, A., Scotto-Lomassese, S., Bernard, J.F., Soiza-Reilly, M., and Gaspar, P. (2016). Conditional anterograde tracing reveals distinct targeting of individual serotonin cell groups (B5-B9) to the forebrain and brainstem. Brain Struct. Funct. *221*, 535–561. https://doi.org/10.1007/s00429-014-0924-4.

51. Bolte, S., and Cordelières, F.P. (2006). A guided tour into subcellular colocalization analysis in light microscopy. J. Microsc. *224*, 213–232. https://doi.org/10.1111/j.1365-2818.2006.01706.x.

52. Kumar, G.A., Sarkar, P., Jafurulla, M., Singh, S.P., Srinivas, G., Pande, G., and Chattopadhyay, A. (2019). Exploring endocytosis and intracellular trafficking of the human serotonin1A receptor. Biochemistry *58*, 2628–2641. https://doi.org/10.1021/acs.biochem.9b00033.

53. Specht, C.G., Izeddin, I., Rodriguez, P.C., El Beheiry, M., Rostaing, P., Darzacq, X., Dahan, M., and Triller, A. (2013). Quantitative nanoscopy of inhibitory synapses: counting gephyrin molecules and receptor binding sites. Neuron *79*, 308–321. https://doi.org/10.1016/j.neuron.2013.05.013.

54. Schneider, C.A., Rasband, W.S., and Eliceiri, K.W. (2012). NIH Image to ImageJ: 25 years of image analysis. Nat. Methods *9*, 671–675.

STAR★METHODS

KEY RESOURCES TABLE

REAGENT or RESOURCE	SOURCE	IDENTIFIER
Antibodies		
mouse anti-HA antibody	Cell Signaling#2367	RRID AB_10691311
rabbit anti-Flag	Cell Signaling#14793	RRID AB_2572291
Cy5-conjugated donkey anti-mouse	Jackson ImmunoResearch#715-175-150	RRID AB_2340819
Cy3-conjugated goat anti-rabbit antibody	Jackson ImmunoResearch#111-165-003	RRID AB_2338000
HA-Tag C29F4 Rabbit mAb Sepharose® Bead Conjugate	Cell Signaling #3956	RRID:AB_10695091
rabbit anti-HA	Cell Signaling#3724	RRID AB_1549585
mouse anti-myc	Cell Signaling#2276	RRID AB_331783
goat anti-mouse-IR800	Advansta# R-05060-250	N/A
goat anti-rabbit-IR700	Advansta# R-05054-250	N/A
Alexa 488 donkey anti- mouse antibody	Jackson ImmunoResearch #715-175-150	RRID AB_2336933
Bacterial and virus strains		
pAAV-EF1A-DIO-WPRE-pA vector	(Belmer et al.[24])	RRID Addgene_39320
Chemicals, peptides, and recombinant proteins		
^{3}H-mesulergine	Perkin-Elmer (Belmer et al.[24])	NET1148250UC
^{3}H-8-OH-DPAT	ISOBIO	ART-0890
BW-723C86	Tocris	Cat. No. 1059
RS-127445	Tocris	Cat. No. 2993
8-OH-DPAT	Tocris	Cat. No. 0529
NAN-190	Tocris	Cat. No. 0553
Critical commercial assays		
IP one HTRF Kit	Cisbio, France	62IPAPEB
Experimental models: Cell lines		
COS-7 cells	LGC STANDARDS	ATCC-CRL-1651pCAGG-
Experimental models: Organisms/strains		
Htr2b^{tm2Lum}/Htr2b^{tm2Lum}	EM:05939, (Belmer et al.[24])	RRID: IMSR_EM:05939
129S2.Cg-Tg(Fev-cre)^{1Esd}/0	IMSR Cat# JAX:012712, (Scott et al.[48])	RRID:IMSR_JAX:012712
Gt(ROSA)26Sor$^{tm1(CAG-EGFP)Fsh}$/Gt(ROSA)26Sor^{+}	MGI Cat# 4420760,	RRID:MGI:4420760
Recombinant DNA		
pCAGG-HA-5-HT$_{2B}$	(Benhadda et al.[29])	
pCAGG-myc-5-HT$_{1A}$	This work	
pCAGG-5-HT$_{2B}$-R-Rluc	(Moutkine et al.[27])	
pCAGG-5-HT$_{1A}$-R-YFP	This work	
pAAV-Flag-5-HT$_{1A}$	This work	
pAAV-HA-5-HT$_{2B}$	This work	
pAAV-Ef1a-DIO-VGAT-WPRE-pA	gift from Bernardo Sabatini	RRID: Addgene_39320
Software and algorithms		
ImageJ	(Schneider et al.[54])	https://imagej.nih.gov/ij/

RESOURCE AVAILABILITY

Lead contact

Further information and requests for resources should be directed to and will be fulfilled by the lead contact, Luc Maroteaux (luc.maroteaux@upmc.fr).

Materials availability

Plasmids generated in this study have been derived from deposited Addgene plasmids: Addgene_39320.

Mouse lines generated in this study have been derived from deposited strains: IMSR_EM:05939; IMSR_JAX:012712; MGI:4420760.

All newly created materials can be accessed by asking the lead contact.

Data and code availability

All data reported in this paper will be shared by the lead contact upon request.

This paper does not report original code.

Any information required to reanalyze the data reported in this paper is available from the lead contact upon request.

EXPERIMENTAL MODEL AND SUBJECT DETAILS

Animals

Floxed mice, *Htr2b*^{tm2Lum}/*Htr2b*^{tm2Lum}, (IMSR Cat# EM:05939, RRID: IMSR_EM:05939) (*Htr2b*$^{lox/lox}$, WT) were generated on a mixed B6; 129S2 background and backcrossed >10 times onto the 129S2 strain. *Htr2b*$^{lox/lox}$ mice were inactivated for *Htr2b* in 5-HT neurons by crossing with *129S2.Cg-Tg(Fev-cre)*^{1Esd}*/0* (IMSR Cat# JAX:012712, RRID:IMSR_JAX:012712) (ePet1-Cre BAC transgenic mice or *Pet1-Cre*$^{+/0}$)[48] generating *129S2.Cg-Pet1-Cre*$^{+/0}$; *Htr2b*^{lox}/*Htr2b*^{lox} conditional knockout mice (2B-KO^{5-HT}) and littermate controls (WT).[24]

For electrophysiology, these strains of mice were further crossed with *Gt(ROSA)26Sor*$^{tm1(CAG-EGFP)Fsh}$/*Gt(ROSA)26Sor*$^{+}$ (MGI Cat# 4420760, RRID:MGI:4420760) (Rosa26; CAG-loxP-STOP- loxP-EGFP or RCE) that after crossing with Pet1-Cre$^{+/0}$ generated (GFP^{5-HT}) that express GFP in Pet1-positive 5-HT neurons only after Cre recombination, and in the presence of floxed allele generated conditional knockout mice (2B-KO^{5-HT}::GFP^{5-HT}) that express GFP but no 5-HT$_{2B}$ in Pet1-positive 5-HT neurons. Males and females mice were used at 25–31 postnatal days.

All mice were bred at our animal facility. Food and water were available *ad libitum*. The temperature was maintained at 21 ± 1°C, under 12/12 h light/dark. Mice were moved to the experimental room in their home cage at least 5 days prior to testing to allow for habituation to the environment.

Sprague-Dawley rat pups used for primary cultures of hippocampal neurons were taken at embryonic day 19 from Janvier labs.

Ethical statement

All experiments involving mice were approved by the local ethical committee, Ethical Committee for Animal Experiments of the Sorbonne University, Charles Darwin C2EA - 05 (authorizations N°APAFIS#28228, and APAFIS#28229). All efforts were made to minimize animal suffering.

METHODS DETAILS

Results are described in accordance with the ARRIVE guidelines for reports in animal research[49] as detailed in Table S2. Numbers of animals for each test are reported in the figure legends.

Viral constructs and stereotaxic injection

To express HA-tagged 5-HT$_{2B}$ and Flag-tagged 5-HT$_{1A}$ specifically in 5-HT neurons, we use a Double floxed Inverse Orientation (DIO) adeno-associated virus (AAV) construct that allows Cre-mediated expression of the transgene (pAAV-EF1A-DIO-WPRE-pA vector; RRID Addgene_39320)[24] (Figure S2). The viruses packaged

into AAV2.9 serotype with titers of 10^{12}-10^{13} viral particles/mL were obtained (UNC Vector Core, Chapel Hill USA). Both AAVs were stereotaxically injected in the B7 raphe nuclei of males or females *Pet1-Cre*$^{+/0}$ mice at 6 weeks of age.[50] They were used 3 weeks after surgery for histological procedures. Respective expression was assessed by immunostaining using a mouse anti-HA antibody (1:500; Cell Signaling#2367, RRID AB_10691311 and a rabbit anti-Flag (1:500; Cell Signaling#14793 RRID AB_2572291 followed by Cy5-conjugated donkey anti-mouse (1.9 μg/mL; Jackson ImmunoResearch#715-175-150, RRID AB_2340819) and the Cy3-conjugated goat anti-rabbit antibody (1.9 μg/mL; Jackson ImmunoResearch#111-165-003, RRID AB_2338000).

Culture of COS-7 cells

COS-7 cells were cultured as monolayers in Dulbecco's modified Eagle's medium (DMEM) (Gibco, Invitrogen) supplemented with 10% fetal calf serum (Biowest) and 1% penicillin/streptomycin (Sigma), in 9-cm dishes (Falcon). Cells were incubated at 37°C in a 5% CO_s atmosphere. Cells 70% confluent in 6-well plates were used for inositol phosphate accumulation and biotinylation experiments, in 24-well plates for membrane binding, in 9-cm dishes for total binding and co-immunoprecipitation/Western-blot and in 96-well plates for BRET experiments. They were transfected with pCAGG vectors using the Genejuice transfection reagent (Merck Millipore) in complete DMEM, according to the manufacturer's instructions. Twenty-four hours before the experimental test, cells were incubated in a serum-free medium.

Co-immunoprecipitation

Co-immunoprecipitation and Western-blotting were performed in COS-7 cells transfected with a total of 10 μg of DNA per 9-cm dishes with a ratio of 7:3 (HA-5-HT_{2B}/empty vector; empty vector/myc-5-HT_{1A}; HA-5-HT_{2B}/myc-5-HT_{1A}) and maintained in culture for three days before harvesting.[27] Cells were centrifuged and suspended in CHAPS lysis buffer (50 mM Tris-HCl, pH 7.4, 0.05 mM EDTA, 10 mM CHAPS, and protease inhibitor cocktail, pH 7.4) and sonicated three times for 30 s. Cells were next solubilized for 5 h at 4°C under gentle agitation. Lysates were centrifuged (20,000 x g) in order to pellet non-solubilized membranes. Protein concentrations in supernatant were measured using the PierceTM Coomassie Protein Assay Kit. Lysates were co-imunoprecipitated with anti-HA beads (HA-Tag C29F4 Rabbit mAb Sepharose Bead Conjugate Cell Signaling #3956 RRID:AB_10695091) overnight at 4°C under gentle agitation. Total lysate and immunoprecipitated proteins were separated by SDS/PAGE onto 10% polyacrylamide gels and transferred electrophoretically to nitrocellulose membranes. Inputs represent 5% of the total protein amount used for immunoprecipitations. Blots were probed with rabbit anti-HA (1:1,000; Cell Signaling#3724, RRID AB_1549585) or mouse anti-myc (1:1,000; Cell Signaling#2276, RRID AB_331783). Antibodies (1:10,000; goat anti-mouse-IR800, Advansta# R-05060-250 and goat anti-rabbit-IR700, Advansta# R-05054-250) were used as secondary antibodies. Immunoreactive bands were detected using the Odyssey software. At least three independent experiments were performed.

Bioluminescence resonance energy transfer (BRET)

BRET assays were performed in 6-well plates. COS-7 cells were transfected with 30–100 ng of plasmid DNA coding for the BRET donor (5-HT_{2B}luc)[27] and an increasing amount of BRET acceptor plasmids (5-HT_{1A}-YFP; from 100 to 4000 ng/well). Twenty-four hours later, the cells were trypsinized (trypsin 0.05% EDTA; Invitrogen) and plated in 96-well plates (50,000 cells/well). The day after, the luciferase substrate, coelenterazine-h, was added in each well at a 5 μM final concentration. Using a Mithras LB940 plate reader, luminescence and fluorescence were then measured simultaneously at 485 and 530 nm, respectively. The BRET ratios were calculated as ((emission at 530 nm/emission at 485 nm)-(background at 530 nm/background at 485 nm)) and were plotted as a function of ((YFP-YFP0)/YFP0)/(Rluc/Rluc0)). The background corresponds to signals in cells expressing the Rluc fusion protein alone under the same experimental conditions. YFP is the fluorescence signal at 530 nm after excitation at 485 nm, and Rluc is the signal at 485 nm after addition of coelenterazine-h. YFP0 and Rluc0 correspond to the values in cells expressing the Rluc fusion protein alone.

Binding experiments

Membrane radioligand binding assay

Membrane binding assays were performed on transfected cells plated in 9-cm dishes.[24] Cells were first washed with PBS, scraped into 10 mL of PBS on ice, and then centrifuged for 5 min at 1,000 g. Cell pellets were dissociated and lysed in 2 mL of binding buffer (50 mM Tris-HCl, 10 mM $MgCl_2$, 0.1 mM EDTA, pH 7.4) and centrifuged for 30 min at 10,000 g. Membrane preparations were then resuspended in binding buffer

to obtain a final concentration of 0.2–0.4 mg of protein/well. Aliquots of membrane suspension (200 µL/well) were incubated with 25 µL/well of ^{3}H-mesulergine or ^{3}H-8-OH-DPAT at a final concentration between 1/2 to 1/10 Kd for each 5-HT receptor, diluted in binding buffer and 25 µL/well of increasing concentrations of heterologous compound. 5-HT_{2B} agonist BW-723C86 (BW) or antagonist RS-127445 (RS), 5-HT_{1A} agonist 8-OH-DPAT or antagonist NAN-190 (NAN) were from Tocris (UK). Competition was performed at concentration between 10^{-11} to 10^{-5} M, diluted in binding buffer in 96-well plates for 60 min at room temperature. Membranes were harvested by rapid filtration onto Whatman GF/B glass fiber filters (Brandell) pre-soaked with cold saline solution and washed three times. Filters were placed in 6-mL scintillation vials and counted. Data in disintegrations/min were converted to femtomoles and normalized to protein content (ranging from 0.1 to 1 mg/well). At least three independent experiments were performed in duplicate.

Non-permeabilized whole cell radioligand binding assay

Cells expressing 5-HT_{2B} and/or 5-HT_{1A} were plated in 24-well plates. Twenty-four hours before the experiment, the cells were incubated in serum-free medium overnight. The next day, the medium was replaced by 400 µL/well of Krebs-Ringer/HEPES buffer (130 mM NaCl, 1.3 mM KCl, 2.2 mM $CaCl_2$, 1.2 mM NaH_2PO_4, 1.2 mM $MgSO_4$, 10 mM HEPES, 10 mM glucose, pH 7.4). Then, 50 µL of [^{3}H]-mesulergine were diluted in Krebs-Ringer/HEPES buffer at a final concentration 1/2 Kd value of 5-HT_{2B}. The radioligand was competed with 50 µL of increasing concentrations of non-radioactive BW, also diluted in Krebs-Ringer/HEPES buffer. Cells were then incubated for 30 min at room temperature and then washed twice on ice with cold PBS. Washed cells were solubilized by the addition of 500 µL of SDS 1%. The next day, 3 mL of scintillation mixture were added to the samples, and the radioactivity was counted. Data in disintegrations/min were converted to femtomoles and normalized to protein content (0.2–0.4 mg of protein/well). At least three independent experiments were performed in duplicate.

Second messenger measurements

COS-7 cells were transfected with 3 µg of DNA (1:1 ratio for co-transfection) in 6-well plates using Genejuice transfecting reagent in complete medium. Twenty-four hours later the cells were trypsinized (trypsin 0.05% EDTA; Invitrogen) and plated in 96-well plates (30,000 cells/well). The next day, the complete medium was replaced by a serum-free medium.

HTRF IP accumulation

The day of the experiment, media were replaced by stimulation buffer with LiCl to prevent IP1 degradation (NaCl, 146 mM, KCl, 4.2 mM, $MgCl_2$, 0.5 mM, $CaCl_2$, 1 mM, HEPES, 10 mM, glucose, 5.5 mM, LiCl, 50 mM, pH7.4). Cells were stimulated during 2 h at 37°C with different concentrations of BW (10^{-11} to 10^{-6} M in stimulation buffer). Stimulation solution was replaced by a lysis buffer (IP one HTRF Kit, Cisbio, France) during 1 h. Lysates were distributed to 384-well plates, and IP was labeled using HTRF reagents. The assay is based on a competitive format involving a specific antibody labeled with terbium cryptate (donor) and IP coupled to d2 (acceptor). After a 1-h incubation with HTRF reagent, the plate was read using Mithras LB940 plate reader according to the manufacturer's instructions. Modelization and EC50 calculation were done using GraphPad Prism 7 software. At least three independent experiments were performed in duplicate.

Surface biotinylation

Surface biotinylation was performed on transfected COS-7 cells. Briefly, cells were initially washed twice in cold PBS and subsequently incubated in PBS containing 1 mg/mL Sulfo-NHS-SS-Biotin for 30 min at 4°C to allow for labeling of all surface membrane proteins. Reaction was stopped by applying a quench solution (100 mM Tris pH 8 in PBS) to remove excess biotin. Biotinylated cells were then homogenized in RIPA buffer containing 25 mM Tris (pH 7.6), 150 mM NaCl, 1% TritonTM X-100, 0.5% sodium deoxycholate, 0.1% SDS, 1 mM NaF and a cocktail of protease inhibitors (Roche). The lysate was centrifuged at 21,000 g to remove nuclei and cellular debris. A small amount of the lysate was removed and constituted the "input" or total lysate. Then, 100 µL of StreptAvidin beads (Thermo Scientific Inc) were added to 40 µg of protein lysate and placed on a rotator at 4°C overnight. Samples were then washed three times in RIPA buffer and a fourth times in RIPA buffer without detergents (25 mM Tris pH 7.6, 150 nM NaCl, 0.5% TritonTM X-100; protease inhibitor); beads were pulled-down after each wash by 1 min centrifugation. Bound proteins were eluted in SDS reducing buffer and heated at 70°C for 5 min.

Western blotting

For co-immunoprecipitation and surface biotinylation experiments, total lysate and immunoprecipitated proteins were separated by SDS/PAGE onto 10% acrylamide gels and transferred electrophoretically to nitrocellulose membranes. Blots were probed with rabbit anti-HA (1:1,000; Cell Signaling#3724, RRID AB_1549585) or mouse anti-myc (1:1,000; Cell Signaling#2276, RRID AB_331783). Secondary antibodies (1:10,000; goat anti-mouse-IR800, Advansta# R-05060-250 and goat anti-rabbit-IR700, Advansta# R-05054-250) were used as secondary antibodies. Immunoreactive bands were detected using the Odyssey software. At least three independent experiments were performed.

Hippocampal neuronal culture and transfection

Hippocampal neurons were prepared from embryonic day 19 Sprague-Dawley rat pups.[29] Dissected tissues were trypsinized (0.25% v/v) and mechanically dissociated in HBSS ($CaCl_2$ 1.2 mM, $MgCl_2$ 0.5 mM, $MgSO_4$ 0.4 mM, KCl 5 mM, KH_2PO_4 0.44 mM, $NaHCO_3$ 4.1 mM, NaCl 138 mM, Na_2HPO4 0.34 mM, D-Glucose 5.5 mM) containing 10 mM HEPES (Invitrogen). Dissociated cells were plated on glass coverslips (Assistent) precoated with 55 μg/mL poly-D,L-ornithine (Sigma-Aldrich) in plating medium composed of MEM supplemented with horse serum (10% v/v; Invitrogen), L-glutamine (2 mM), and Na pyruvate (1 mM, Invitrogen) at a density of 3.4×10^4 cells/cm^2 and maintained in humidified atmosphere containing 5% CO_2 at 37°C. After attachment for 2–3 h, cells were incubated in maintenance medium that consists of Neurobasal medium supplemented with B27, L-glutamine (2 mM), and antibiotics (Invitrogen). Each week, one-third of the culture medium volume was renewed. Neuronal transfection with plasmids encoding HA-5-HT_{2B}, Myc-5-HT_{1A} and eGFP were performed at 13–14 DIV using Transfectin (Bio-Rad), according to the instructions of the manufacturer (DNA/lipofectant ratio of 1:3), with 1.5 μg of plasmid DNA per 20-mm well. The following ratio of plasmid DNA was used in co-transfection experiments: 1:0.3:0.2 μg for HA-5-HT_{2B}/Myc-5-HT_{1A}/eGFP. Experiments were performed 7–10 days after transfection.

Immunostaining

The total (membrane plus intracellular) pools of HA-5-HT_{2B} and myc-5-HT_{1A} were revealed with immunocytochemistry in fixed and permeabilized cells, whereas the membrane pool was done in non-permeabilized cells. To label the total pool of receptors, cells were fixed for 10 min at room temperature in paraformaldehyde (PFA; 4% w/v; Sigma) and sucrose (20% w/v; Sigma) solution in PBS. Cells were then washed in PBS, and permeabilized for 4 min with Triton X-100 (0.25% v/v) in PBS. After these washes, non-specific staining was blocked for 30 min with goat serum (20% v/v; Invitrogen) in PBS. Neurons were then incubated for 1 h with either rabbit anti-HA antibodies (1:500; Cell Signaling #3724, RRID AB_1549585) or mouse anti-myc antibodies (1:500; Cell Signaling #2276, RRID AB_331783) in PBS supplemented with Goat Serum (GS) (3% v/v). Cells were then washed three times and incubated for 45 min with Cy5-conjugated donkey anti-mouse or Alexa 488 donkey anti-mouse antibodies (1.9 μg/mL; Jackson ImmunoResearch # 715-175-150, RRID AB_2340819 or #715-175-150, RRID AB_2336933) or the Cy3-conjugated goat anti-rabbit antibodies (1.9 μg/mL; Jackson ImmunoResearch # 111-165-003, RRID AB_2338000) in PBS-goat serum blocking solution, washed, and mounted on slides with Mowiol 4–88 (48 mg/mL). In experiments using BW723C86, 5-HT, or 8-OH-DPAT, drugs were diluted in imaging medium and applied to neurons for 10 or 20 min at 1 μM final concentration before fixation and immunolabeling. The imaging medium consisted of phenol red-free MEM supplemented with glucose (33 mM), HEPES (20 mM), glutamine (2 mM), Na+-pyruvate (1 mM), and B27 (1X, Invitrogen). Sets of neurons to be compared were labeled and imaged simultaneously.

Fluorescence image acquisition and cluster analyses

Fluorescence image acquisition and analyses were performed on images obtained with a Leica SP5 confocal microscope using the LAS-AF program (Leica).[29] Stacks of 16–35 images were acquired using a 100× objective with an interval of 0.2 μm and an optical zoom of 1.5. Image exposure time was determined on bright cells to avoid pixel saturation. All images from a given culture were then acquired with the same exposure time. Quantifications of clusters were performed using MetaMorph software (Roper Scientific) on projections (sum of intensity) of confocal optical sections. For each cell, a region of interest (ROI) was chosen.

For 5-HT_{2B} cluster analysis, images were first flattened background filtered (kernel size, 3 × 3 × 2) to enhance cluster outlines, and a user-defined intensity threshold was applied to select clusters and avoid their coalescence. Thresholded clusters were binarized, and binarized regions were outlined and

transferred onto raw data to determine the mean 5-HT_{2B} cluster number, area and fluorescence intensity. For quantification, clusters comprising at least 3 pixels were considered. The dendritic surface area of regions of interest was measured to determine the number of clusters per 10 μm^2. Due to the variability between cultures, the number of clusters in each culture was normalized to the respective control values, allowing for comparisons between cultures.

As the 5-HT_{1A} presents an expression pattern in small clusters, the average fluorescent intensity per pixel was measured in a defined ROI. For each culture, we analyzed 7–12 dendrites per experimental condition. A total of about 10 neurons were analyzed per condition from three to five independent cultures. The experimenter was blind to the culture treatment.

Quantitative colocalization analysis

Two-channel confocal microscopic images were analyzed for colocalization with the Manders' colocalization coefficient, using the JACoP plug-in[51] for ImageJ (National Institute of Health, Bethesda, MD). In order to facilitate analysis, 100 × 100 μm areas were arbitrarily selected close to the midline DR. This analysis was performed on three independent viral co-infections. Similar results were obtained in each independent experiment. Image stacks were converted to binary images with the threshold function of the JACoP plug-in and manually adjusted. The Manders' coefficient determines the degree (from 0 to 1) of overlap between red (5-HT_{2B}) and green (5-HT_{1A}) channels.[52]

STORM imaging

STochastic Optical Reconstruction Microscopy (STORM) imaging was conducted on an inverted N-STORM Nikon Eclipse Ti microscope equipped with a 100× oil-immersion TIRF objective (NA 1.49) and an Andor iXon Ultra 897 EMCCD camera using 405 and 638 nm lasers from Coherent. Movies of 30,000 frames were acquired at frame rates of 50 Hz. The z position was maintained during acquisition by a Nikon Perfect Focus System and multicolor fluorescent microspheres (Tetraspeck, Invitrogen) were used as markers to register long-term acquisitions and correct for lateral drifts. Single-molecule localization and 2D image reconstruction was conducted as described in[53] by fitting the point-spread function of spatially separated fluorophores to a 2D Gaussian distribution. The surface of clusters and the densities of molecules per μm^2 were measured in reconstructed 2D images through cluster segmentation based on detection densities. The threshold to define the border was set to 1000 detections/μm^2. All pixels containing <2 detections were considered empty, and their intensity value was set to 0. The intensity of pixels with 2 detections was set to 1. The resulting binary image was analyzed with the function "regionprops" of MATLAB to extract the surface area of each cluster identified by this function. Density was calculated as the total number of detections in the pixels belonging to a given cluster, divided by the area of the cluster.

Electrophysiology

For patch clamp experiments, 260 μm-thick brain coronal slices were prepared from GFP^{5-HT} mice (control) and 2B-KO^{5-HT}::GFP^{5-HT} mice at 4 weeks (25–31 postnatal days) that express GFP only in Pet1-positive 5-HT neurons. The brain extraction and slicing was performed in ice-cold (0°C–4°C) oxygenated (95% O_2-5% CO_2) solution containing 110 mM choline chloride, 2.5 mM KCl, 25 mM glucose, 25 mM $NaHCO_3$, 1.25 mM NaH_2PO_4, 0.5 mM $CaCl_2$, 7 mM $MgCl_2$, 11.6 mM L-ascorbic acid, and 3.1 mM sodium pyruvate. Slices were then stored in artificial cerebro-spinal fluid (aCSF) containing 125 mM NaCl, 2.5 mM KCl, 25 mM glucose, 25 mM $NaHCO_3$, 1.25 mM NaH_2PO_4, 2 mM $CaCl_2$, and 1 mM $MgCl_2$ (pH 7.2, maintained by continuous bubbling with 95% O_2-5% CO_2). Slices were incubated in aCSF at 32°C for 20 min and then at room temperature (20°C–25°C). Slices were transferred to the recording chamber where they were continuously superfused with oxygenated aCSF (30°C–32°C). To block synaptic transmission, we added to the aCSF 6-cyano-7-nitroquinoxaline-2,3-dione (CNQX; 10 μM, Hello Bio), D-2-amino-5-phosphonopentanoic acid (D-APV; 50 μM, Hello Bio) and SR95531 hydrobromide (GABAzine, 10 μM, Hello Bio). We also used (±) 8-hydroxy-2-(di-*n*-propylamino)tetralin hydrobromide (8-OH-DPAT; 30 nM, SIGMA) and Apamin (20 nM, Hello Bio) to activate 5-HT_{1A} and block SK channels, respectively. Current clamp and voltage-clamp recordings were performed with pipettes (5- to 7-MΩ resistance) prepared from borosilicate glass (BF150-86-10; Harvard Apparatus) using a DMZ pipette puller (Zeitz). Pipettes were filled with an intracellular solution containing 105 mM K-gluconate, 10 mM HEPES, 10 mM phosphocreatine-Na, 4 mM ATP-Na_2, and 30 mM KCl (pH 7.25, adjusted with KOH). The input resistance (Rinput) was computed using a 10-mV hyperpolarizing step from a holding potential of −65 mV (50 ms). Current-clamp and voltage-clamp recordings were performed using an EPC-10 amplifier (HEKA Elektronik). Data acquisition was performed

using Patchmaster software (Heka Elektronik). The liquid junction potential (−5 mV) was left uncorrected. Signals were sampled at 20 kHz and filtered at 4 kHz. Data analysis was performed using Igor Pro (Wavemetrics). Statistical analyses were performed using Prism (GraphPad). The normality of data distribution was tested using Shapiro–Wilk's test. Unpaired two-tailed t-tests (for normally distributed datasets) or Mann–Whitney tests (for non-normally distributed datasets) were used for comparisons between two groups. For multiple comparisons, we used two-way ANOVA followed by Sidak's test. Values of $p < 0.05$ were considered statistically significant.

QUANTIFICATION AND STATISTICAL ANALYSIS

Experimental design and statistical analysis

Statistical analyses were performed using GraphPad Prism 7 software. Starting from our experience in previous publications,[24,29] we calculated the standard deviation of each group of animals for each test as well as the differences between the means of these groups. By setting the type I and II error risks at 5 and 20%, respectively, the size of the groups were determined by calculating the statistical power using the G*Power software version 3.1.9.6. To ensure reproducibility, when relevant, experiments were performed at least three times independently. To avoid litter bias in the mouse experiments, experimental groups are composed of animals from different litters randomly distributed using Graphpad software. All analyses were conducted with blinding to the experimental condition. Putative outliers were determined by the ROUT method. Data are presented as bars and the line at the mean ± S.E.M. (standard error of the mean). Comparisons between two groups following a normal distribution were analyzed using two-tailed unpaired t-test with or without Welch's correction. Normality was assessed using the D'Agostino & Pearson omnibus normality test. All data normally distributed for more than two groups were examined by either ordinary two-way ANOVA followed by Tukey's multiple comparisons or repeated measure two-way ANOVA followed by Sidak's multiple comparisons test. Data not passing the normality test were analyzed using the Kruskal-Wallis test followed by Dunn's multiple comparison test. $p < 0.05$ was predetermined as the threshold for statistical significance (See Table S1 for full statistical analysis).

The Table S1 provides the full statistical analysis.